

JET PROPULSION LABORATORY

SIRTF IPF REPORT

JPL ID002121

October 20, 2003

**SIRTF INSTRUMENT POINTING FRAME
KALMAN FILTER EXECUTION SUMMARY**

IPF RUN NUMBER: 002121

REPORT TYPE: IOC EXECUTION (COARSE)

PRIME FRAME: MIPS_SED_center (121)

INFERRRED FRAMES: (113) (114) (116) (117) (122) (123) (125) (126)

IPF TEAM

Autonomy and Control Section (345)

Jet Propulsion Laboratory

California Institute of Technology

4800 Oak Grove Drive

Pasadena, CA 91109

Contents

1 IPF EXECUTION SUMMARY	5
2 IPF INPUT FILE HISTORY	10
3 IPF EXECUTION RESULTS	11
3.1 IPF EXECUTION OUTPUT PLOTS	11
3.2 IPF OUTPUT DATA (IF MINI FILE)	34
3.3 IPF EXECUTION LOG	38
4 COMMENTS	42

List of Figures

1.1 A-priori and a-posteriori IPF frames	5
1.2 A-priori and a-posteriori IPF frames (ZOOMED)	9
2.1 Scenario Plot	10
3.1 TPF coords of measurements and a-priori predicts	13
3.2 Oriented PixelCoords of measurements and a-priori predicts	13
3.3 Oriented (W,V) PixelCoords of A-Priori Prediction Error Quiver Plot	14
3.4 A-priori prediction error (Science Centroids)	14
3.5 Oriented PixelCoords of measurements and a-priori predicts (PCRS only)	15
3.6 Oriented PixelCoords of measurements and a-priori predicts (Zoomed, PCRS only) . .	15
3.7 Oriented (W,V) PixelCoords of A-Priori PCRS Prediction Error Quiver Plot	16
3.8 A-priori PCRS prediction error	16
3.9 IPF execution convergence, chart 1	17
3.10 IPF execution convergence, chart 2	17
3.11 Parameter uncertainty convergence	18
3.12 IPF parameter symbol table	18
3.13 KF parameter error sigma plots	19
3.14 LS parameter error sigma plot	19
3.15 KF and LS parameter error sigma plot	20
3.16 Oriented PixelCoords of meas. and a-posteriori predicts	21
3.17 Oriented PixelCoords of meas. and a-posteriori predicts (attitude corrected)	21

3.18	KF innovations with (o) and w/o (+) attitude corrections	22
3.19	Histograms of science a-posteriori residuals (or innovations)	22
3.20	KF innovations with (o) and w/o (+) attitude corrections (PCRS)	23
3.21	Histograms of PCRS a-posteriori residuals (or innovations)	23
3.22	A-Posteriori Science Centroid Prediction Error Quiver (Att. Cor.)	24
3.23	Normalized A-Posteriori Science Centroid Prediction Errors	24
3.24	A-Posteriori PCRS Prediction Errors Quiver (Att. Cor.)	25
3.25	Normalized A-Posteriori PCRS Prediction Errors	25
3.26	W-axis KF innovations and 1-sigma bound	26
3.27	V-axis KF innovations and 1-sigma bound	26
3.28	Array plot with (solid) and w/o (dashed) optical distortion corrections	27
3.29	Optical Distortion Plot: total (x5 magnification)	27
3.30	Optical Distortion Plot: constant plate scales (x5 magnification)	28
3.31	Optical Distortion Plot: linear plate scale (x5 magnification)	28
3.32	Optical Distortion Plot: gamma terms (x5 magnification)	29
3.33	Estimated attitude corrections (Body frame)	30
3.34	Estimated attitude error sigma plot (Body frame)	30
3.35	Thermo-mechanical boresight drift (equiv. angle in (W,V) coords)	31
3.36	Thermo-mechanical boresight drift (equiv. angle in Body frame)	31
3.37	Gyro drift bias contribution (equiv. rate in (W,V) coords)	32
3.38	Gyro drift bias contribution (equiv. angle in (W,V) coords)	32
3.39	Gyro drift bias contribution (equiv. angle in Body frame)	33

List of Tables

1.1	IPF filter input files	6
1.2	IPF filter execution configuration	6
1.3	IPF filter execution mask vector assignment	6
1.4	IPF calibration error summary ([arcsec], 1-sigma, radial)	7
1.5	Measurement prediction error summary (1-sigma)	7
1.6	IPF Brown angle summary	8
2.1	IPF input file editing status	10
3.1	Table of figures I (IPF run)	11

3.2 Table of figures II (IPF run)	12
---	----

1 IPF EXECUTION SUMMARY

This report summarizes the SIRTF Instrument Pointing Frame (IPF) Kalman Filter execution associated with run file: RN002121. In particular, this Focal Point Survey calibrates the instrument: MIPS_SED_center (121), as part of the IOC Coarse Survey. The main calibration results from the IPF filter execution have been documented in IF002121 typically stored in the mission archive DOM collection IPF_IF. This report only summarizes the main aspects of the run, and does not substitute for the full information contained in the IF file.

Section 1 summarizes the filter execution results. The filter configurations are tabulated in Table 1.2 and the mask vector assignments are tabulated in Table 1.3. A total of 8 state parameters are estimated in this run. The overall End-to-End pointing performances are tabulated in Table 1.4. The prediction residuals throughout the estimation processes are tabulated in Table 1.5. Section 3 summarizes resulting plots, a mini summary of the IF IPF output file, and the execution log. Section 4 captures the user comments that are specific to this particular run.

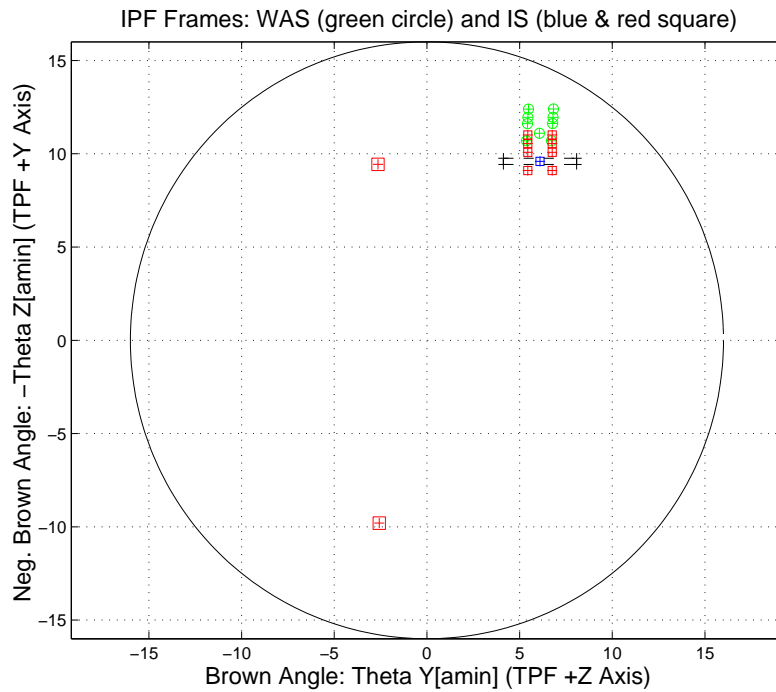


Figure 1.1: A-priori and a-posteriori IPF frames

RAW	FINAL (After Editing)
AA001121	AA001121
AS001121	AS001121
CA002121	CA002121
CB002121	CB002121
CS002121	CS002121

Table 1.1: IPF filter input files

EXECUTION CONFIGURATION ITEM	CURRENT STATUS
IPF Filter Version Used	IPF.V2.0.0C
Frame Table Version Used	BodyFrames_SPC_08a
Scan-Mirror Employed?	NO
IPF Filter Mode	LITE-MODE(2):STA
SLIT-MODE Operation	ENABLED
Kalman Filter Operation	ENABLED
Least-Squares Data Analysis	ENABLED
IBAD Screening	ENABLED
User-Specified Data Editing	DISABLED
Total Number of Iterations	25
LS Residual Sigma Scale	1.34447956E+000
Total Number of Maneuvers	6

Table 1.2: IPF filter execution configuration

Con. Plate Scale			Γ Dependent				Γ^2 Dependent				Linear Plate Scale						Mirror			
a_{00}	b_{00}	c_{00}	a_{10}	b_{10}	c_{10}	d_{10}	a_{20}	b_{20}	c_{20}	d_{20}	a_{01}	b_{01}	c_{01}	d_{01}	e_{01}	f_{01}	α	β		
1	2	3	4	5	6	7	8	9	10	11	12	13	14	15	16	17	18	19		
0	0	0	0	0	0	0	0	0	0	0	0	0	0	0	0	0	0	0		
IPF (T)			Alignment R						Gyro Drift Bias											
θ_1	θ_2	θ_3	a_{rx}	a_{ry}	a_{rz}	b_{rx}	b_{ry}	b_{rz}	c_{rx}	c_{ry}	c_{rz}	b_{gx}	b_{gy}	b_{gz}	c_{gx}	c_{gy}	c_{gz}			
20	21	22	23	24	25	26	27	28	29	30	31	32	33	34	35	36	37			
0	1	1	1	1	1	1	1	1	0	0	0	0	0	0	0	0	0			

Table 1.3: IPF filter execution mask vector assignment

FOCAL PLANE SURVEY ANALYSIS: IOC Coarse Survey.

INSTRUMENT NAME: MIPS_SED_center NF: 121

PIX2RADW: 4.79222664E-005 [rad/pixel] = 9.8847E+000 [arcsec/pixel]

PIX2RADV: 4.79222664E-005 [rad/pixel] = 9.8847E+000 [arcsec/pixel]

FRAME	DESCRIPTION	IPF ¹	SF ²	TOTAL	REQ
121(P)	MIPS_SED_center	26.4390	0.0855	26.4392	1.15
113(I)	MIPS_SED_5	26.4390	0.0855	26.4392	N/A
114(I)	MIPS_SED_6	26.4390	0.0855	26.4392	N/A
116(I)	MIPS_SED_7	26.4390	0.0855	26.4392	N/A
117(I)	MIPS_SED_8	26.4390	0.0855	26.4392	N/A
122(I)	MIPS_SED_1	26.4390	0.0855	26.4392	N/A
123(I)	MIPS_SED_2	26.4390	0.0855	26.4392	N/A
125(I)	MIPS_SED_3	26.4390	0.0855	26.4392	N/A
126(I)	MIPS_SED_4	26.4390	0.0855	26.4392	N/A

Table 1.4: IPF calibration error summary ([arcsec], 1-sigma, radial)

RMS METRIC	A PRIORI ³	A POSTERIORI ³	ATT. CORRECTED ⁴	UNITS
Radial	14.7641	0.2007	0.0019	arcsec
W-Axis	0.3624	0.1952	0.0001	arcsec
V-Axis	14.7597	0.0466	0.0019	arcsec
Radial	1.4936	0.0203	0.0002	pixels
W-Axis	0.0367	0.0198	0.0000	pixels
V-Axis	1.4932	0.0047	0.0002	pixels

Table 1.5: Measurement prediction error summary (1-sigma)

¹IPF filter removes systematic pointing errors due to: thermomechanical alignment drift (Body to TPF), gyro bias and bias drift, centroiding error, attitude error, and optical distortion. IPF SIGMA presented here is “Scaled” by the Least Squares Scale factor. The Least Squares Scale Factor was: 1.344480. It is assumed that the gyro Angle Random Walk contribution is captured with the Least Squares scaling. The gyro ARW contribution can be approximately calculated as 0.0837 arcseconds, given that ARW = 100 $\mu\text{deg}/\sqrt{\text{hr}}$, with 5.834000e+002 second Maneuver time (max), and 6 independent Maneuvers.

²Gyro Scale Factor(GSF) assumes 95 ppm error over 0.250 degree maneuver.

³This can be interpreted as estimate of ”pixel to sky” pointing reconstruction error if no science data is used.

⁴This can be interpreted as estimate of achieved S/I centroiding error

IPF BROWN ANGLE SUMMARY					
FRAME TABLE USED: BodyFrames_SPC_08a					
NF	NAME	WAS	IS	CHANGE	UNIT
121	theta_Y	+6.073000	+6.099911	+0.026911	arcmin
121	theta_Z	-11.098000	-9.595594	+1.502406	arcmin
121	angle	-0.000000	+0.000044	+0.000044	deg
113	theta_Y	+6.830000	+6.758890	-0.071110	arcmin
113	theta_Z	-12.398000	-11.007261	+1.390739	arcmin
113	angle	+0.000000	+0.000044	+0.000044	deg
114	theta_Y	+5.479000	+5.440933	-0.038067	arcmin
114	theta_Z	-12.391000	-11.007261	+1.383739	arcmin
114	angle	+0.000000	+0.000044	+0.000044	deg
116	theta_Y	+6.723000	+6.758889	+0.035889	arcmin
116	theta_Z	-10.701000	-9.102260	+1.598740	arcmin
116	angle	-0.000000	+0.000044	+0.000044	deg
117	theta_Y	+5.373000	+5.440932	+0.067932	arcmin
117	theta_Z	-10.695000	-9.102261	+1.592739	arcmin
117	angle	+0.000000	+0.000044	+0.000044	deg
122	theta_Y	+6.781000	+6.758890	-0.022110	arcmin
122	theta_Z	-11.623000	-10.077261	+1.545739	arcmin
122	angle	+0.000000	+0.000044	+0.000044	deg
123	theta_Y	+5.430000	+5.440933	+0.010933	arcmin
123	theta_Z	-11.616000	-10.077261	+1.538739	arcmin
123	angle	+0.000000	+0.000044	+0.000044	deg
125	theta_Y	+6.802000	+6.758890	-0.043110	arcmin
125	theta_Z	-11.957000	-10.548928	+1.408072	arcmin
125	angle	-0.000000	+0.000044	+0.000044	deg
126	theta_Y	+5.451000	+5.440933	-0.010067	arcmin
126	theta_Z	-11.951000	-10.548928	+1.402072	arcmin
126	angle	-0.000000	+0.000044	+0.000044	deg

Table 1.6: IPF Brown angle summary

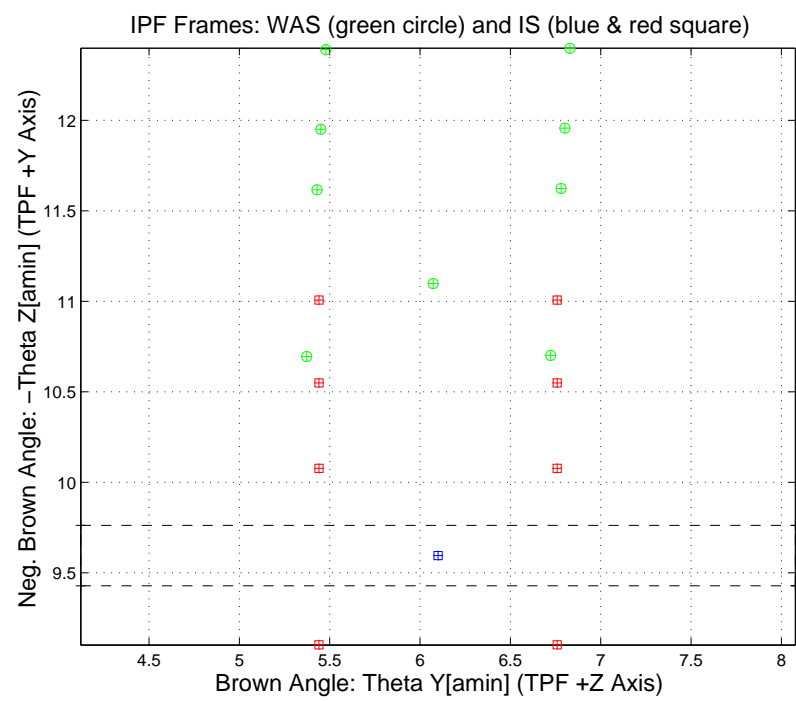


Figure 1.2: A-priori and a-posteriori IPF frames (ZOOMED)

2 IPF INPUT FILE HISTORY

WAS	SIZE	IS	SIZE	REMOVED	PATCHED
AA001121	UNCHANGED	AA001121	UNCHANGED	0	0
CA002121	UNCHANGED	CA002121	UNCHANGED	0	N/A
CB002121	UNCHANGED	CB002121	UNCHANGED	0	N/A

Table 2.1: IPF input file editing status

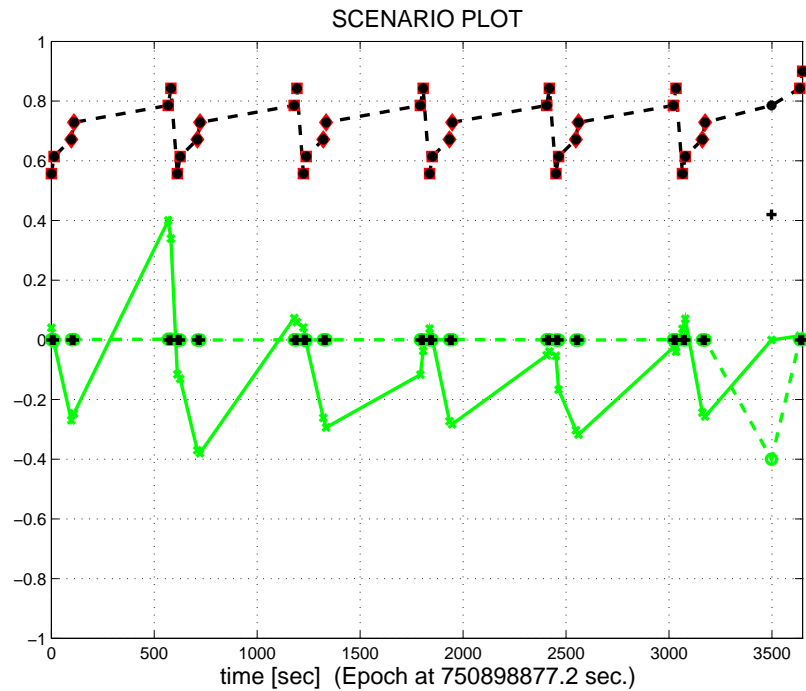


Figure 2.1: Scenario Plot

3 IPF EXECUTION RESULTS

3.1 IPF EXECUTION OUTPUT PLOTS

This subsection summarizes the IPF filter results. As shown in Table 3.1, the output plots are segmented to three groups: predicted performance, post-run results and IPF trending plots.

FIGURE NO.	DESCRIPTION
Predicted performance prior to IPF run	
Figure 3.1	Meas. and a-priori predicts in TPF coords
Figure 3.2	Meas. and a-priori predicts in Oriented Pixel Coords including rectangular array boundary approximation
Figure 3.3	A-Priori Prediction Error Quiver Plot in Oriented Pixel Coords including rectangular array boundary approximation
Figure 3.4	A-priori prediction error
Figure 3.5	Oriented Pixel Coords of measurements and a-priori predicts (PCRS only)
Figure 3.6	Oriented Pixel Coords of measurements and a-priori predicts (Zoomed, PCRS only)
Figure 3.7	Oriented (W,V) Pixel Coords of A-Priori PCRS Prediction Error Quiver Plot
Figure 3.8	A-priori PCRS prediction error
IPF filter performance (post run results)	
Figure 3.9	IPF execution convergence, chart 1: (top) normalized residual error vs. iteration number and (bottom) norm of effective parameter corrections
Figure 3.10	IPF execution convergence, chart 2: parameter correction size vs. iteration number
Figure 3.11	Parameter uncertainty convergence: square-root of diagonal elements of covariance matrix vs. maneuver number
Figure 3.12	IPF parameter symbol table
Figure 3.13	KF parameter error sigma plot (a-priori-dashed, a-posteriori-solid). Includes true parameter errors (FLUTE runs only)
Figure 3.14	LS parameter error sigma plot. Includes true parameter errors (FLUTE runs only)
Figure 3.15	KF and LS parameter errors sigma plot (Figure 3.13 & Figure 3.14 combined)
Figure 3.16	Measurements and a-posteriori predicts in Oriented Pixel Coords including rectangular array boundaries (a-priori-dashed, a-posteriori-solid)
Figure 3.17	Attitude corrected meas. and a-posteriori predicts in Oriented Pixel Coords including rectangular array boundaries (a-priori-dashed, a-posteriori-solid)

Table 3.1: Table of figures I (IPF run)

FIGURE NO.	DESCRIPTION
IPF filter performance (post run results) - CONTINUE	
Figure 3.18	KF innovations with (o) and w/o (+) attitude corrections
Figure 3.19	Histograms of science a-posteriori residuals (or innovations)
Figure 3.20	KF innovations with (o) and w/o (+) attitude corrections (PCRS)
Figure 3.21	Histograms of PCRS a-posteriori residuals (or innovations)
Figure 3.22	A-Posteriori Science Centroid Prediction Error Quiver (Att. Cor.)
Figure 3.23	Normalized A-Posteriori Science Centroid Prediction Errors
Figure 3.24	A-Posteriori PCRS Prediction Errors Quiver (Att. Cor.)
Figure 3.25	Normalized A-Posteriori PCRS Prediction Errors
Figure 3.26	W-axis KF innovations and 1-sigma bound
Figure 3.27	V-axis KF innovations and 1-sigma bound
Figure 3.28	Array plot with (solid) and w/o (dashed) optical distortion corrections
Figure 3.29	Optical Distortion Plot: total (x5 magnification)
Figure 3.30	Optical Distortion Plot: constant plate scales (x5 magnification)
Figure 3.31	Optical Distortion Plot: linear plate scale (x5 magnification)
Figure 3.32	Optical Distortion Plot: gamma terms (x5 magnification)
IPF parameter trending plots	
Figure 3.33	Estimated attitude corrections (Body frame)
Figure 3.34	Estimated attitude error sigma plot (Body frame)
Figure 3.35	Systematic error attributed to thermo-mechanical boresight drift (equiv. angle in (W,V) coords)
Figure 3.36	Systematic error attributed to thermo-mechanical boresight drift (equiv. angle in Body frame)
Figure 3.37	Systematic error attributed to gyro drift bias (equiv. rate in (W,V) coords)
Figure 3.38	Systematic error attributed to gyro drift bias (equiv. angle in (W,V) coords)
Figure 3.39	Systematic error attributed to gyro drift bias (equiv. angle in Body frame)

Table 3.2: Table of figures II (IPF run)

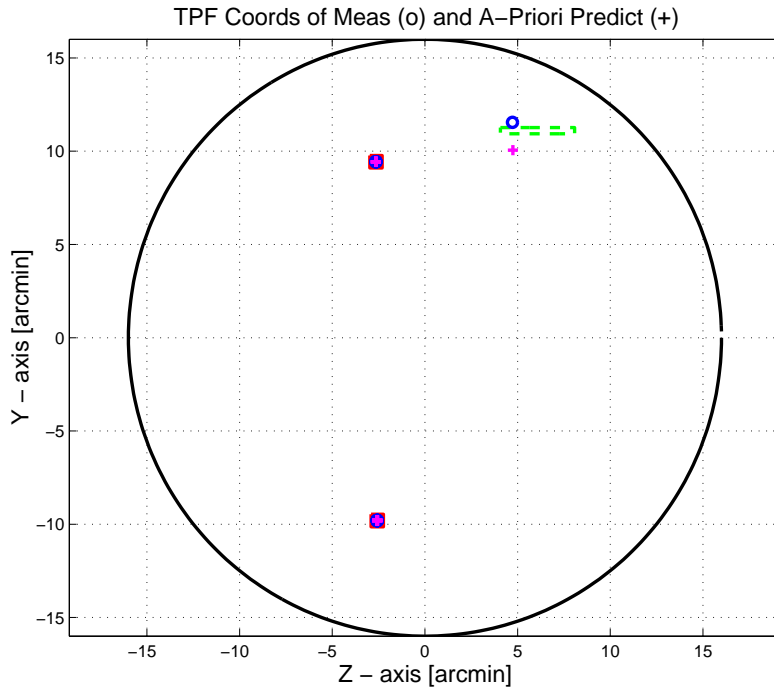


Figure 3.1: TPF coords of measurements and a-priori predicts

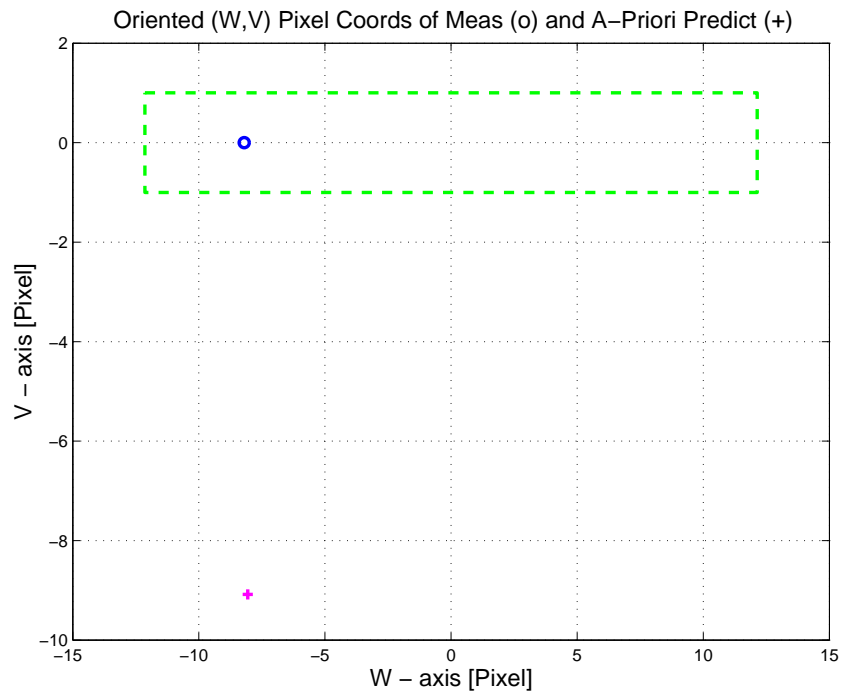


Figure 3.2: Oriented Pixel Coords of measurements and a-priori predicts

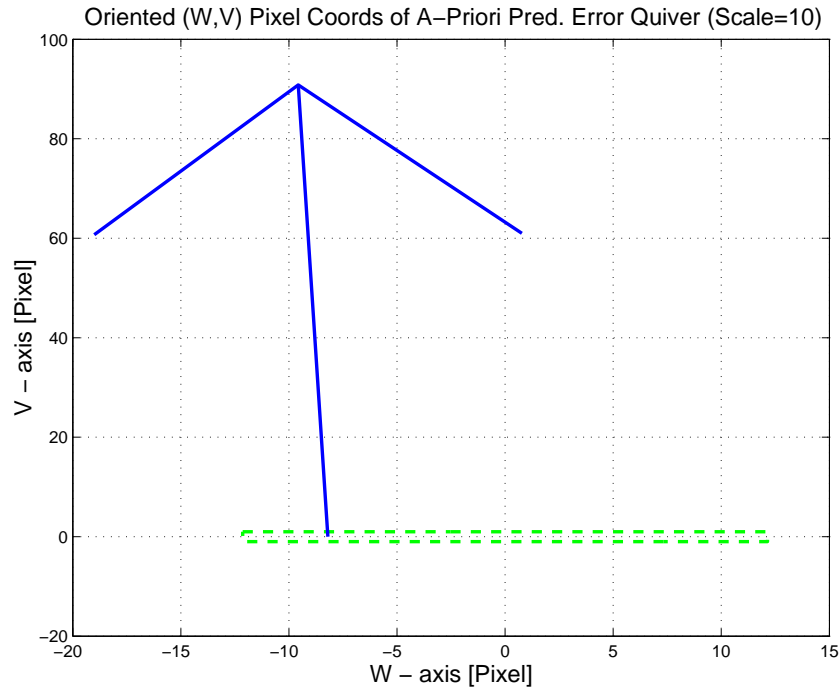


Figure 3.3: Oriented (W,V) Pixel Coords of A-Priori Prediction Error Quiver Plot

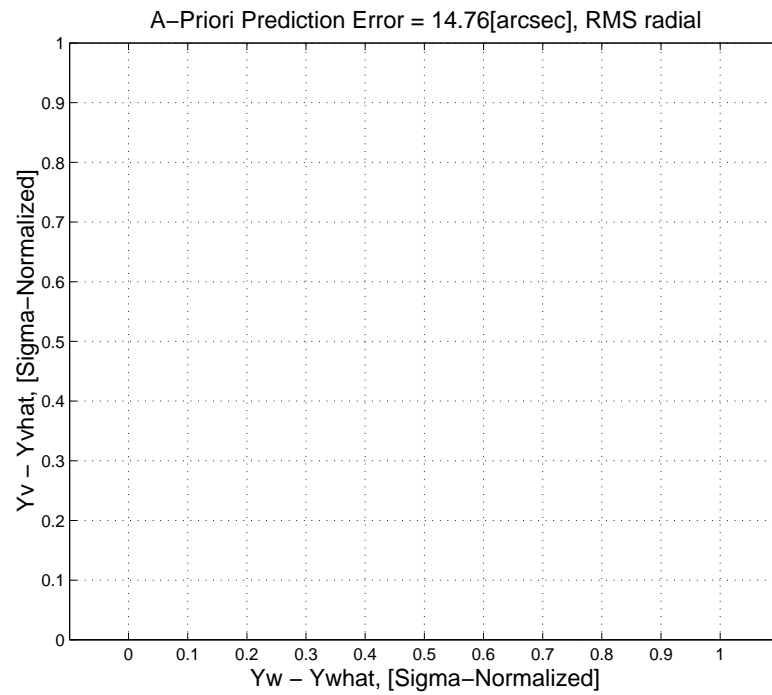


Figure 3.4: A-priori prediction error (Science Centroids)

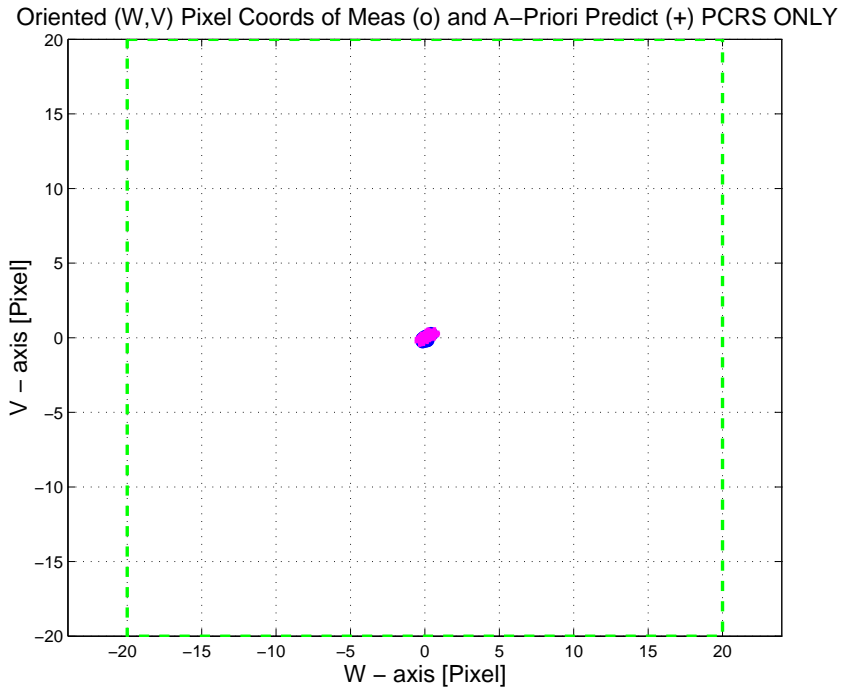


Figure 3.5: Oriented Pixel Coords of measurements and a-priori predicts (PCRS only)

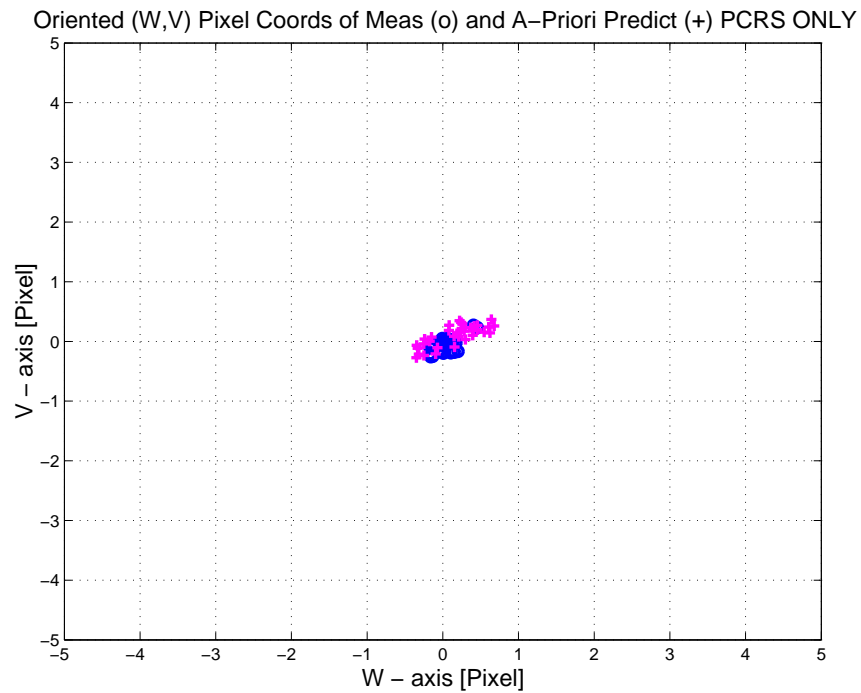


Figure 3.6: Oriented Pixel Coords of measurements and a-priori predicts (Zoomed, PCRS only)

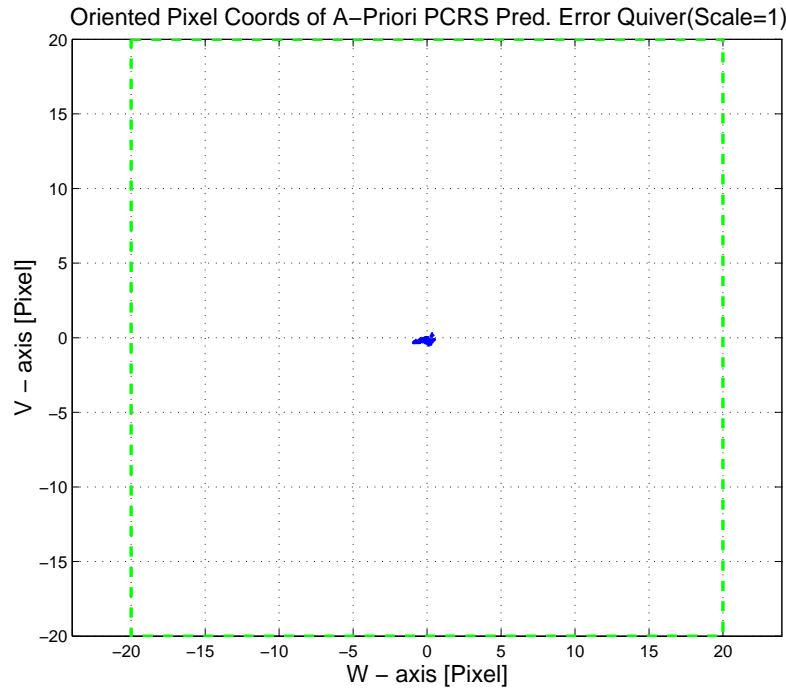


Figure 3.7: Oriented (W,V) Pixel Coords of A-Priori PCRS Prediction Error Quiver Plot

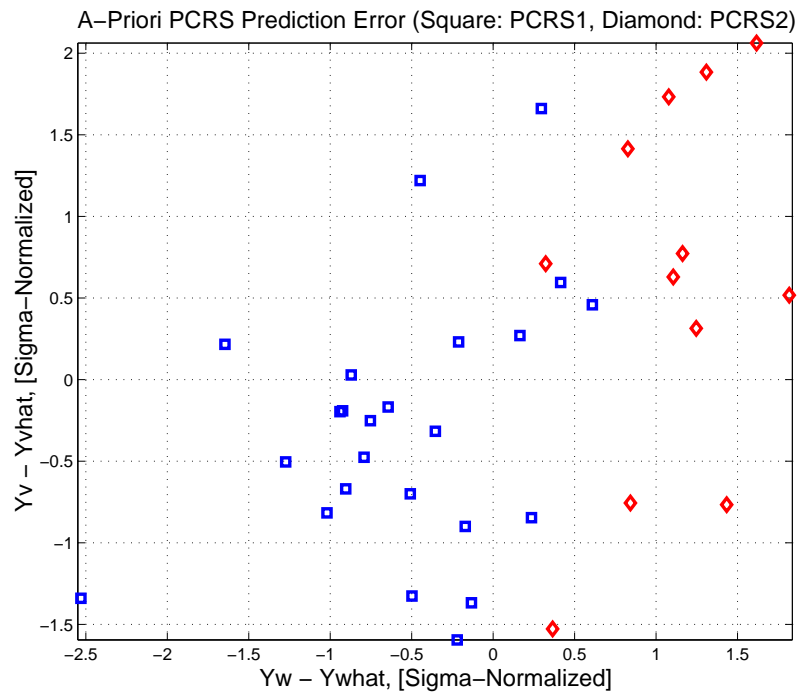


Figure 3.8: A-priori PCRS prediction error

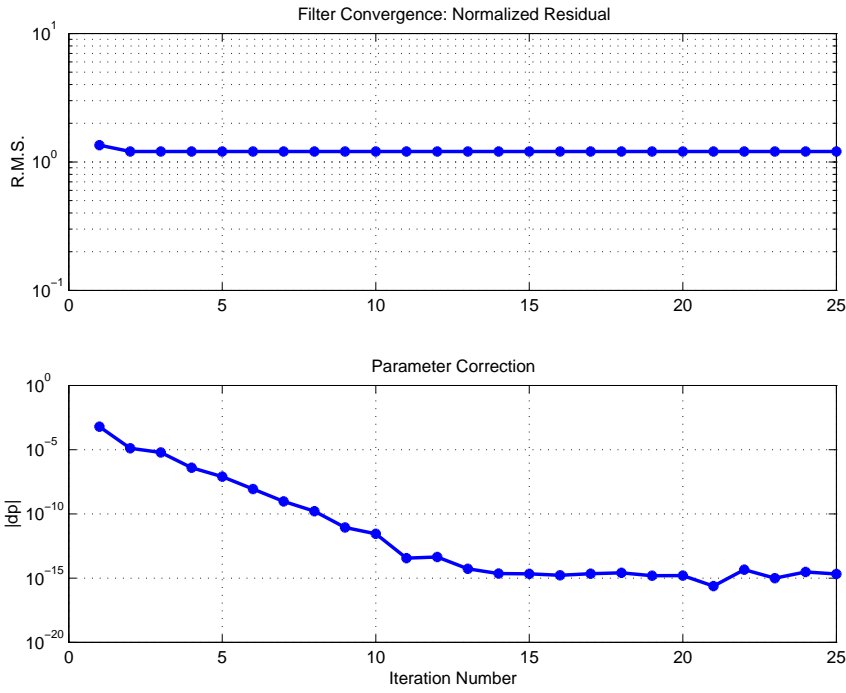


Figure 3.9: IPF execution convergence, chart 1

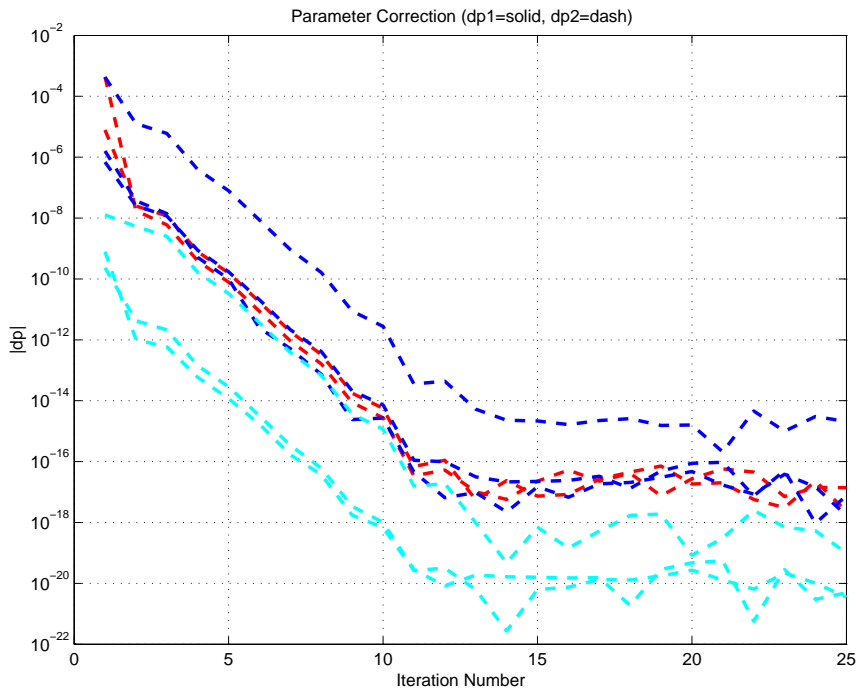


Figure 3.10: IPF execution convergence, chart 2

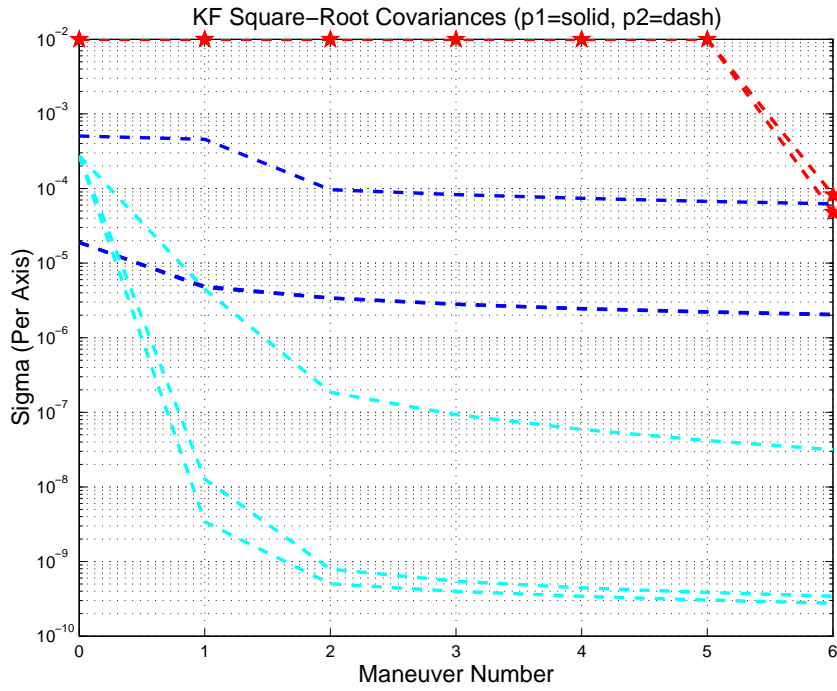


Figure 3.11: Parameter uncertainty convergence

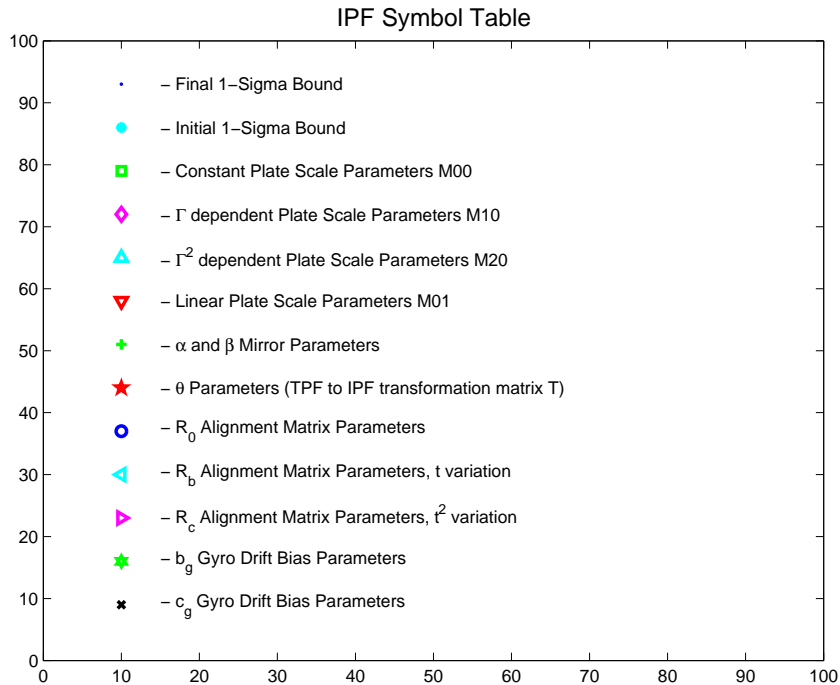


Figure 3.12: IPF parameter symbol table

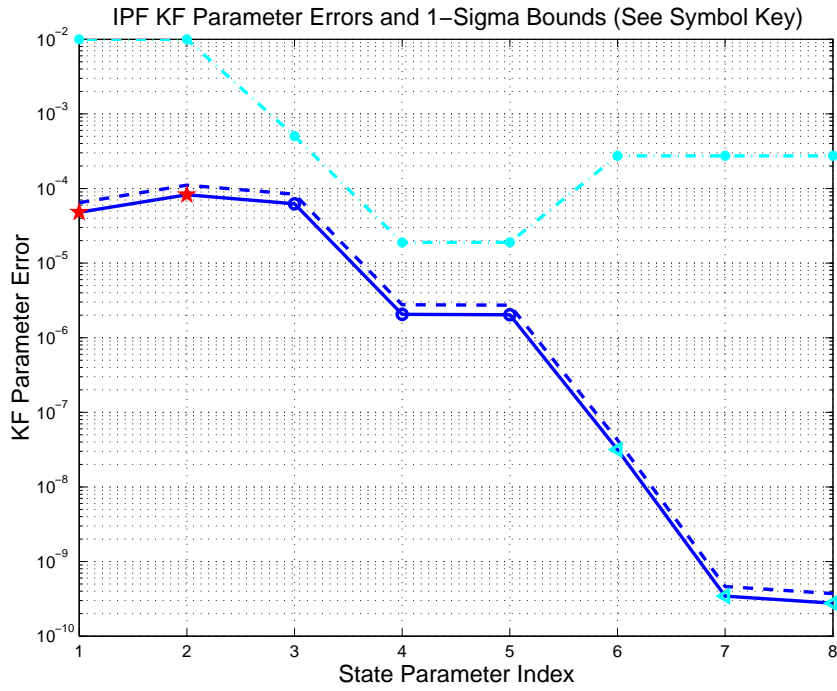


Figure 3.13: KF parameter error sigma plots

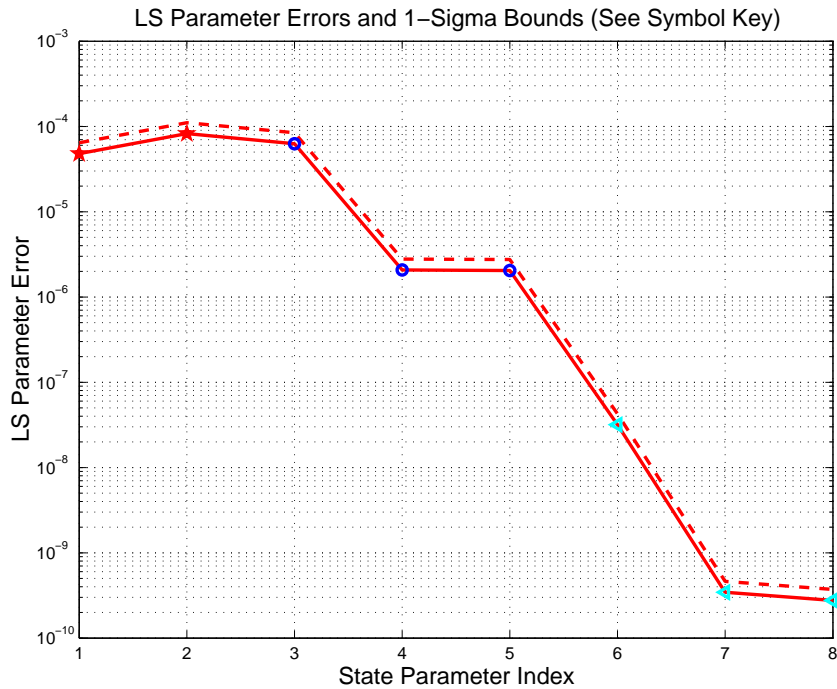


Figure 3.14: LS parameter error sigma plot

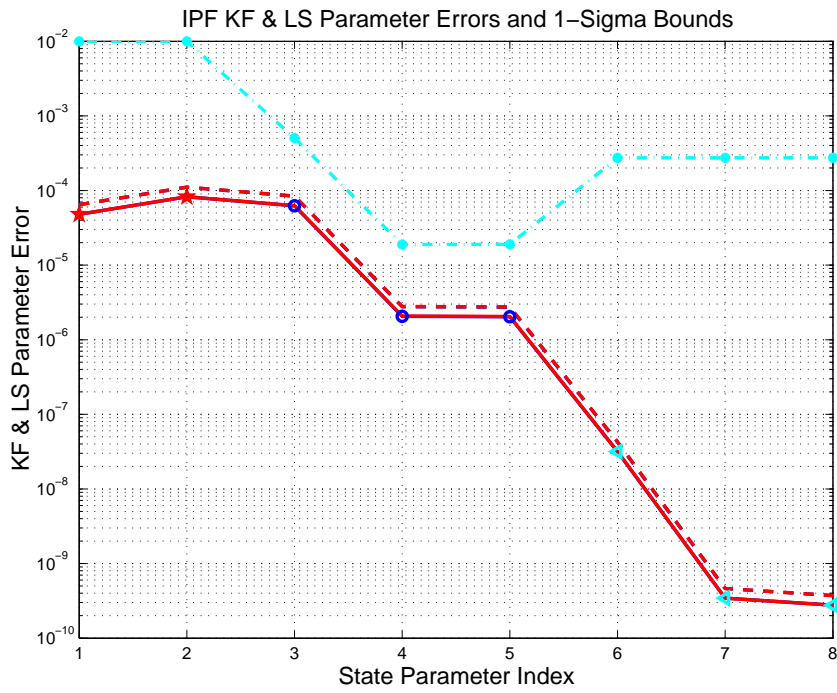


Figure 3.15: KF and LS parameter error sigma plot

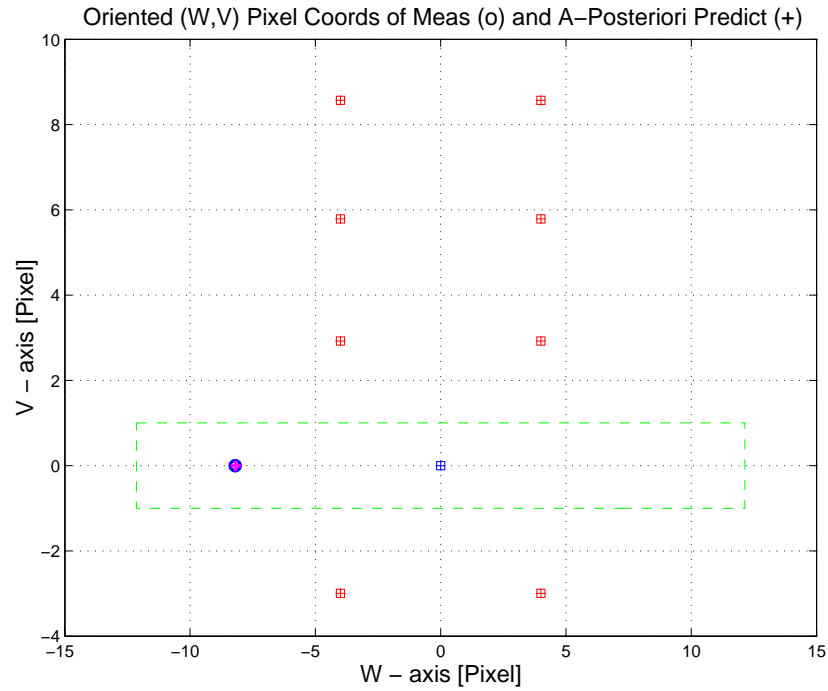


Figure 3.16: Oriented Pixel Coords of meas. and a-posteriori predicts

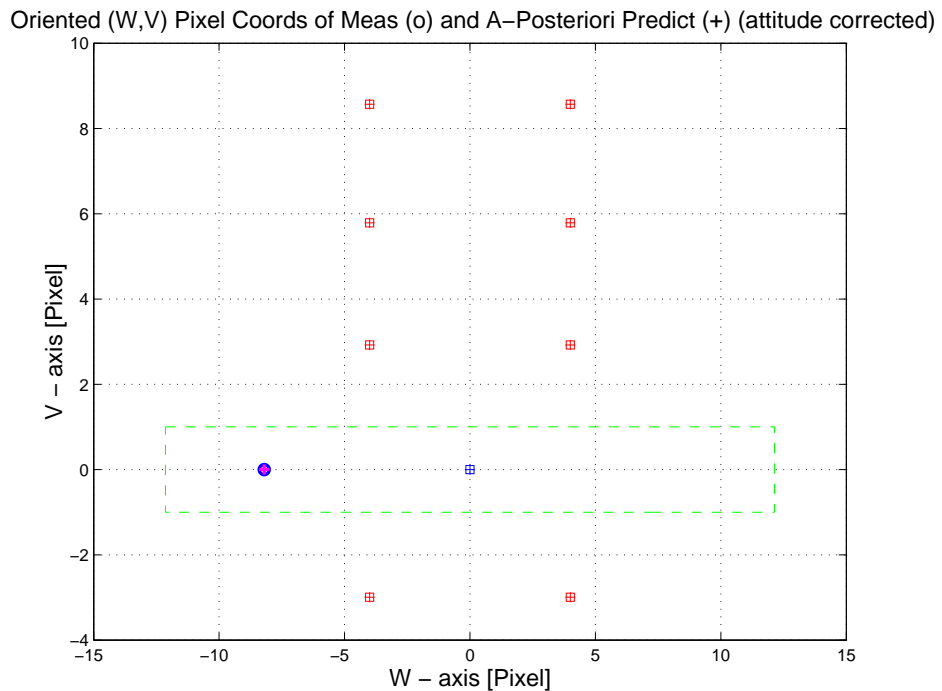


Figure 3.17: Oriented Pixel Coords of meas. and a-posteriori predicts (attitude corrected)

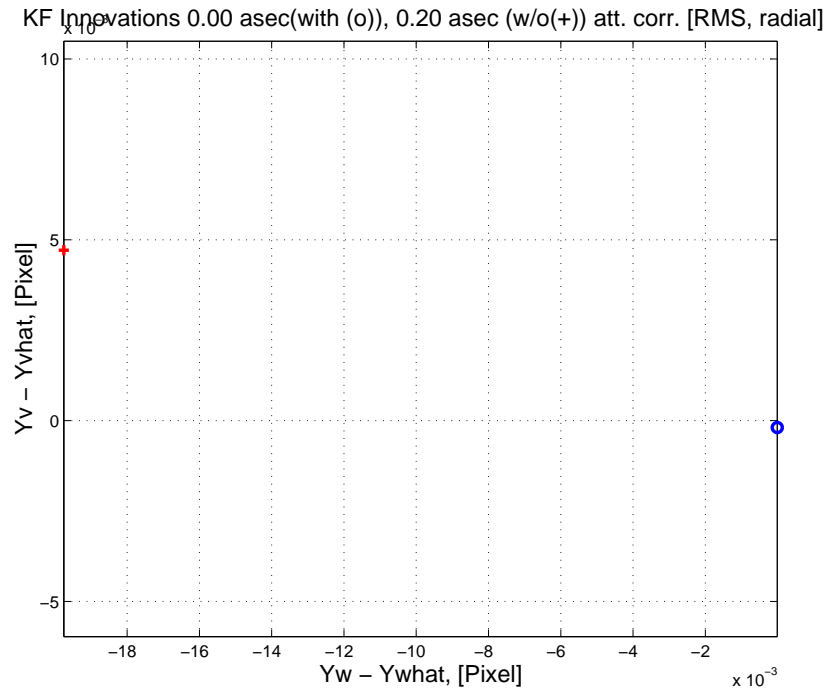


Figure 3.18: KF innovations with (o) and w/o (+) attitude corrections

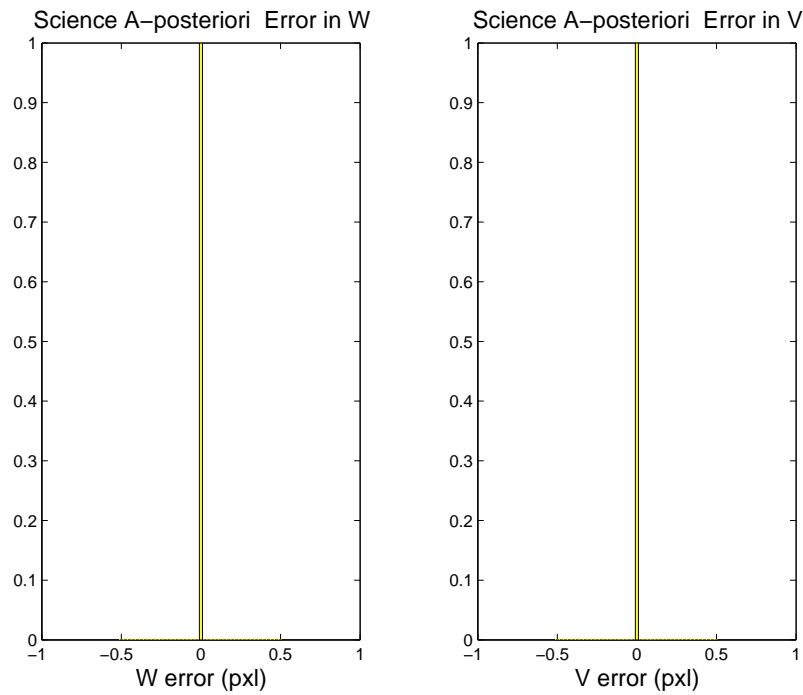


Figure 3.19: Histograms of science a-posteriori residuals (or innovations)

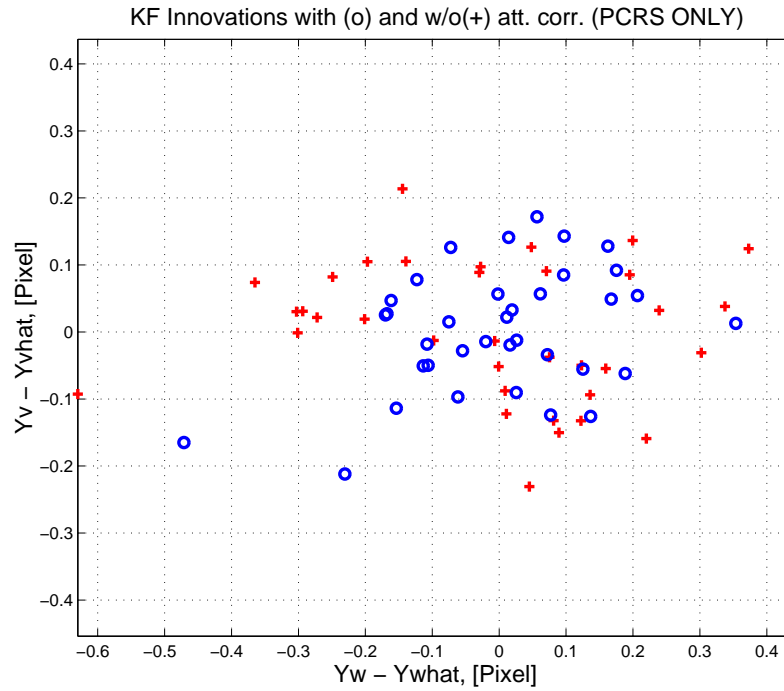


Figure 3.20: KF innovations with (o) and w/o (+) attitude corrections (PCRS)

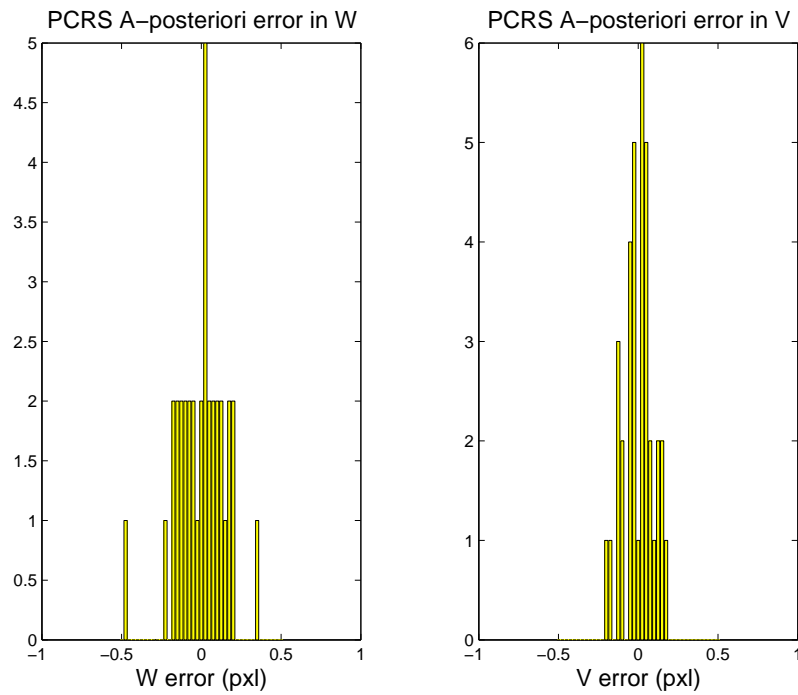


Figure 3.21: Histograms of PCRS a-posteriori residuals (or innovations)

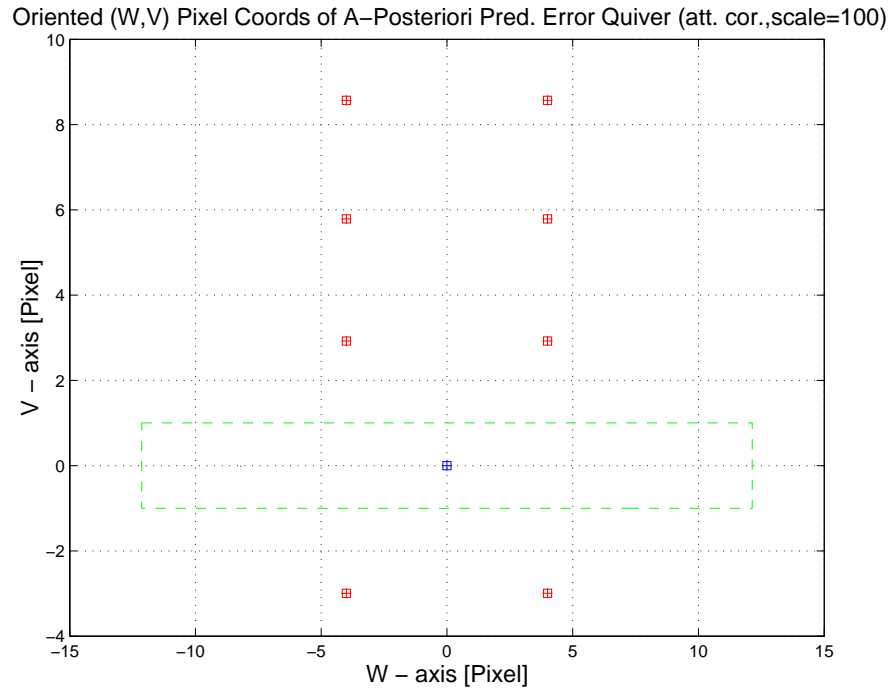


Figure 3.22: A-Posteriori Science Centroid Prediction Error Quiver (Att. Cor.)

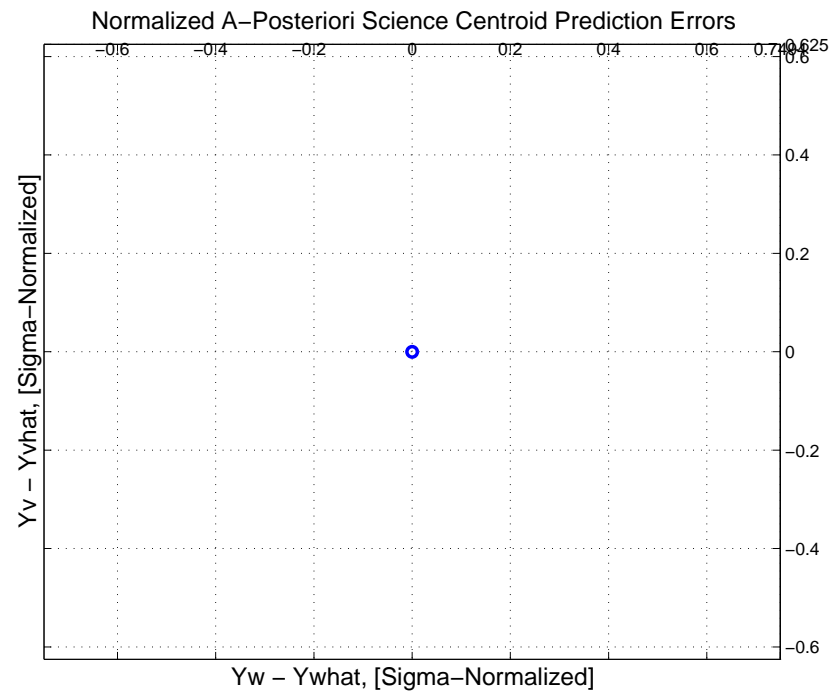


Figure 3.23: Normalized A-Posteriori Science Centroid Prediction Errors

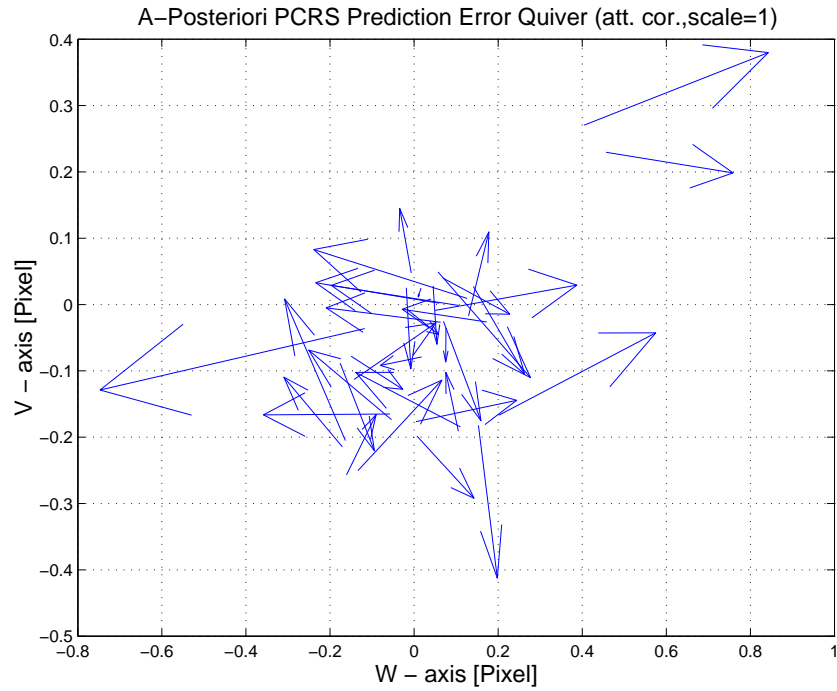


Figure 3.24: A-Posteriori PCRS Prediction Errors Quiver (Att. Cor.)

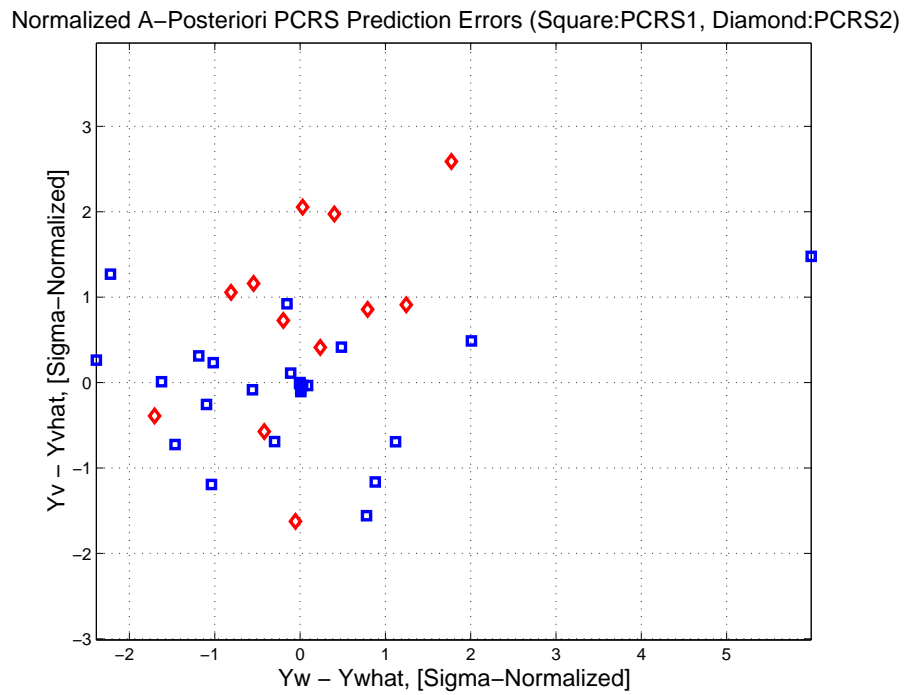


Figure 3.25: Normalized A-Posteriori PCRS Prediction Errors

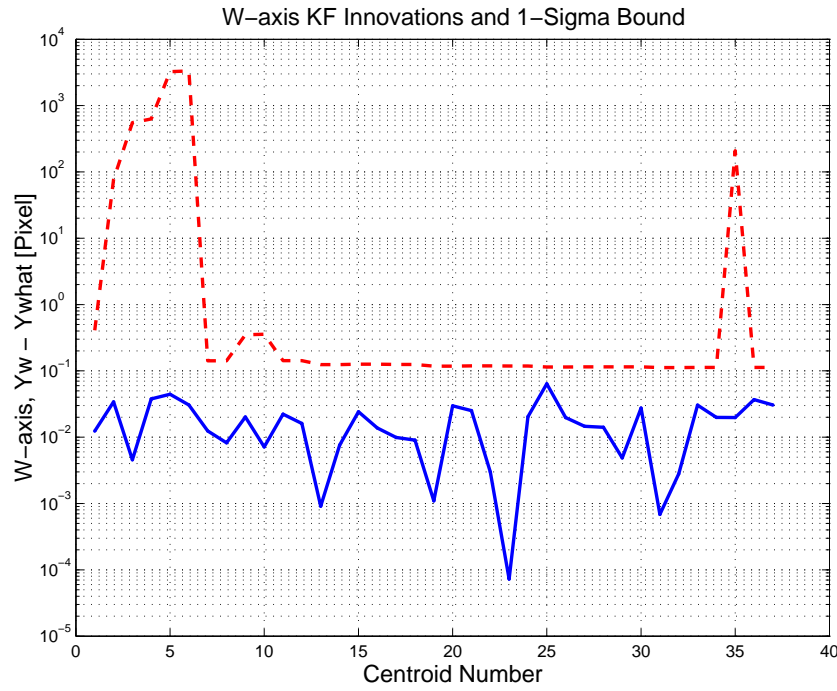


Figure 3.26: W-axis KF innovations and 1-sigma bound

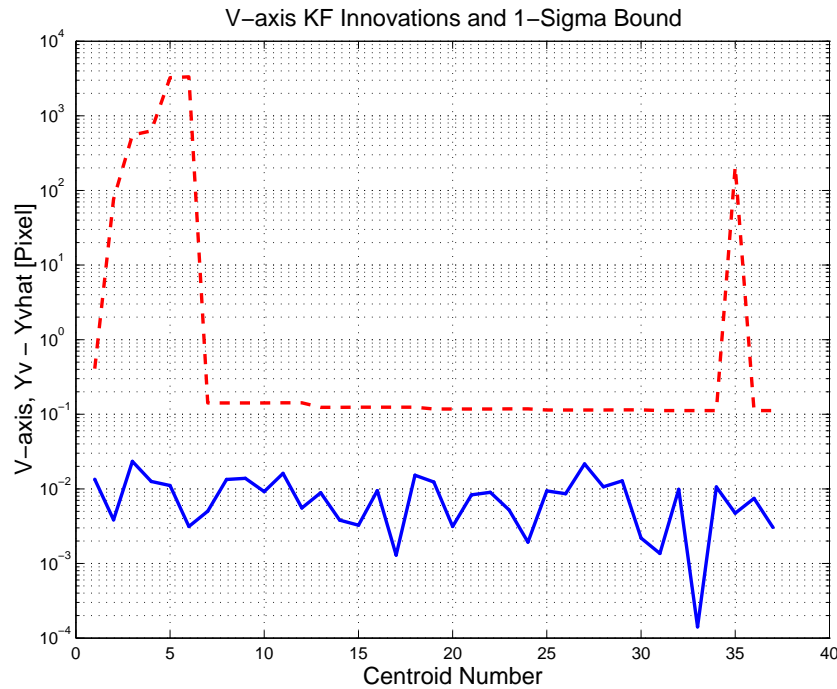


Figure 3.27: V-axis KF innovations and 1-sigma bound

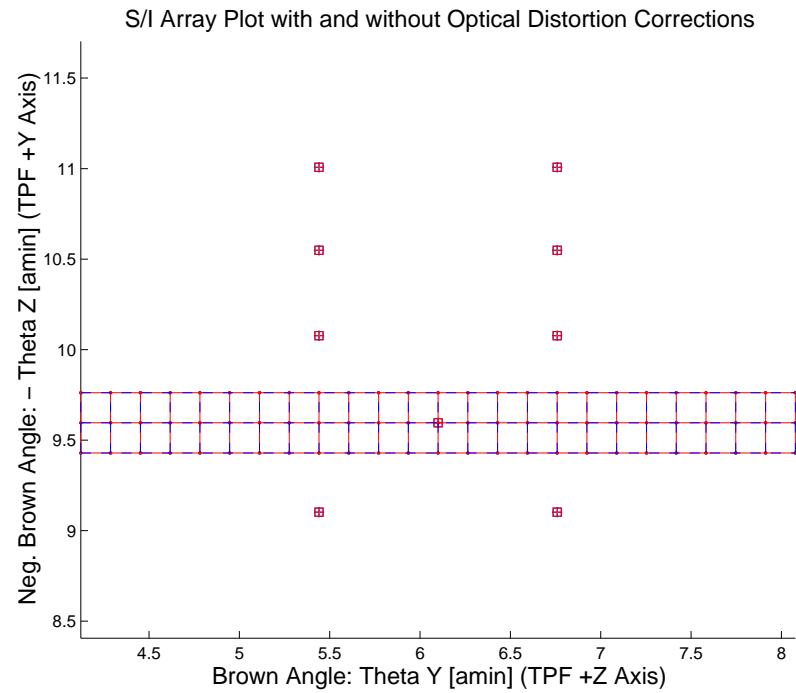


Figure 3.28: Array plot with (solid) and w/o (dashed) optical distortion corrections

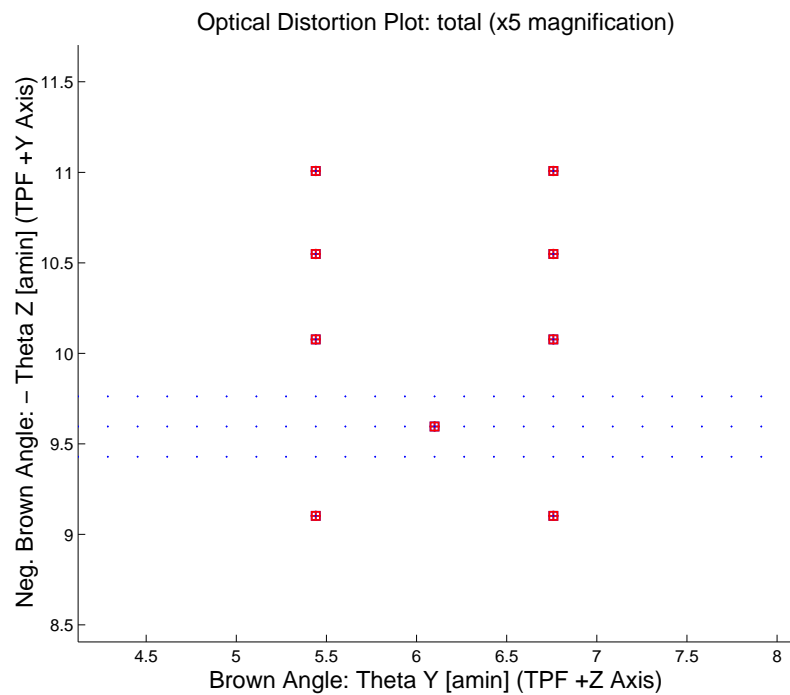


Figure 3.29: Optical Distortion Plot: total (x5 magnification)

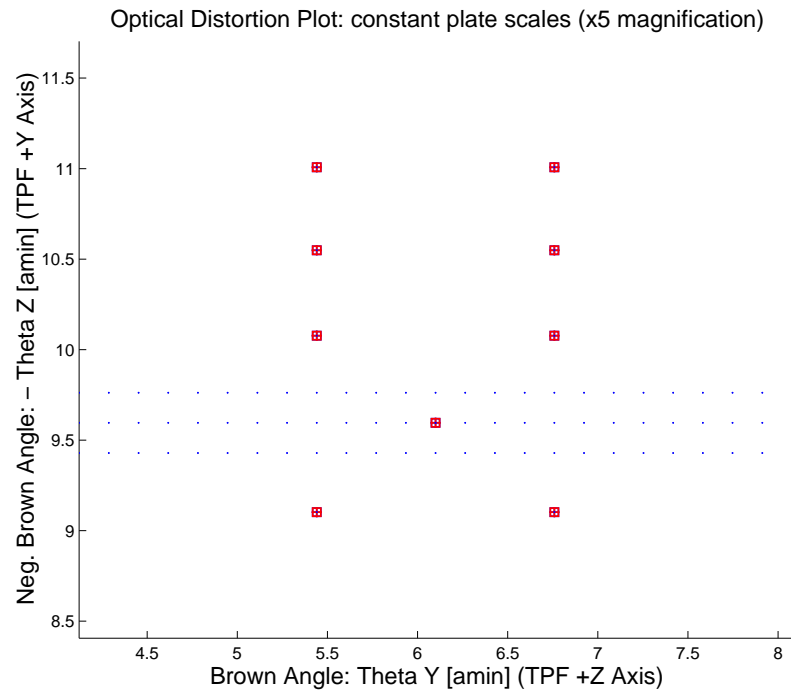


Figure 3.30: Optical Distortion Plot: constant plate scales (x5 magnification)

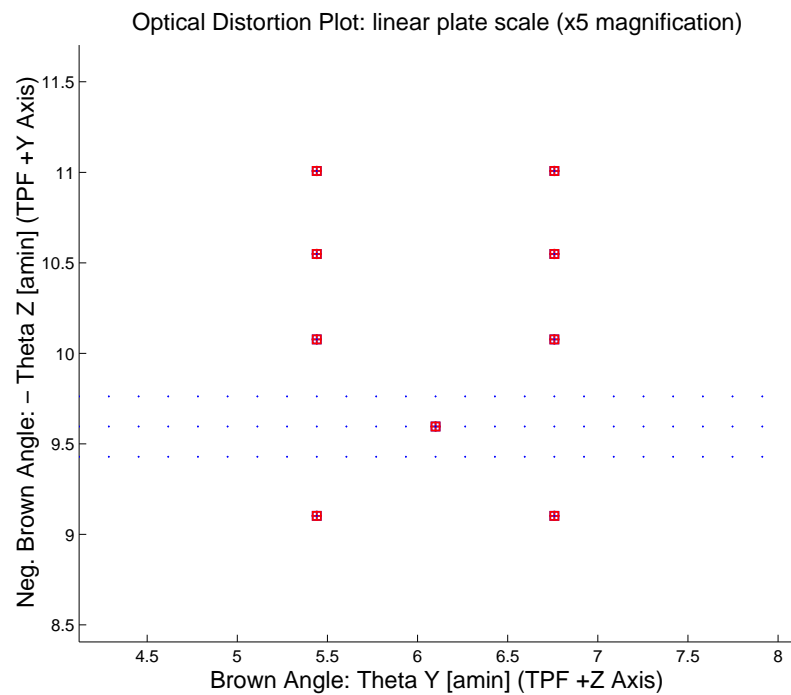


Figure 3.31: Optical Distortion Plot: linear plate scale (x5 magnification)

Opt. Dist. Plot: Γ depdt; $\Gamma = 0.00000e+000$ in blue and $\Gamma = 0.00000e+000$ in red (x5 magn)

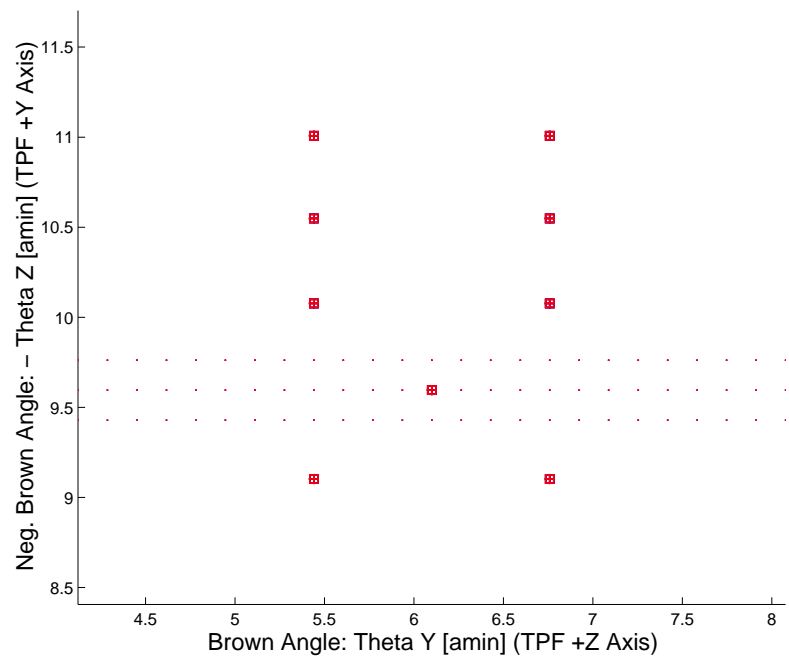


Figure 3.32: Optical Distortion Plot: gamma terms (x5 magnification)

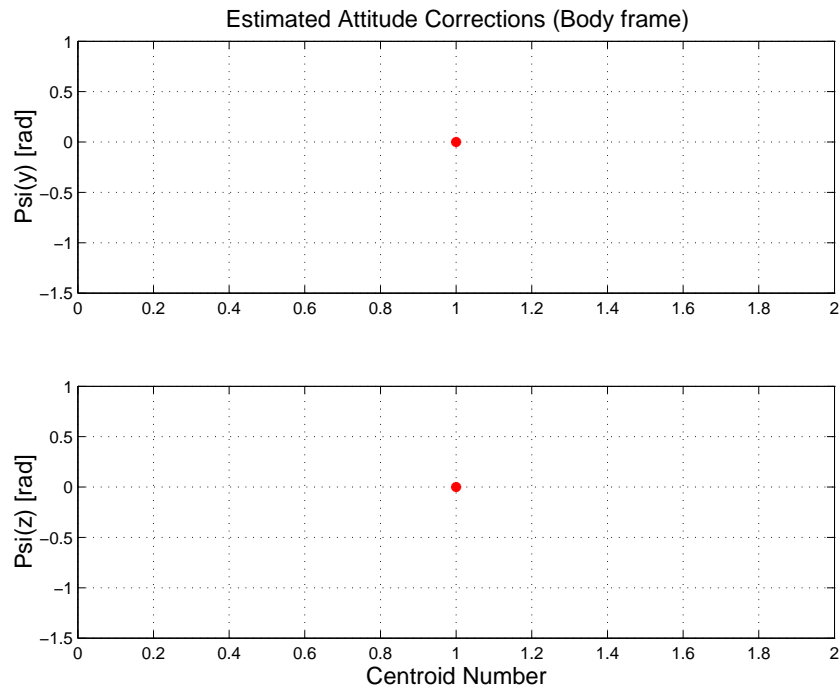


Figure 3.33: Estimated attitude corrections (Body frame)

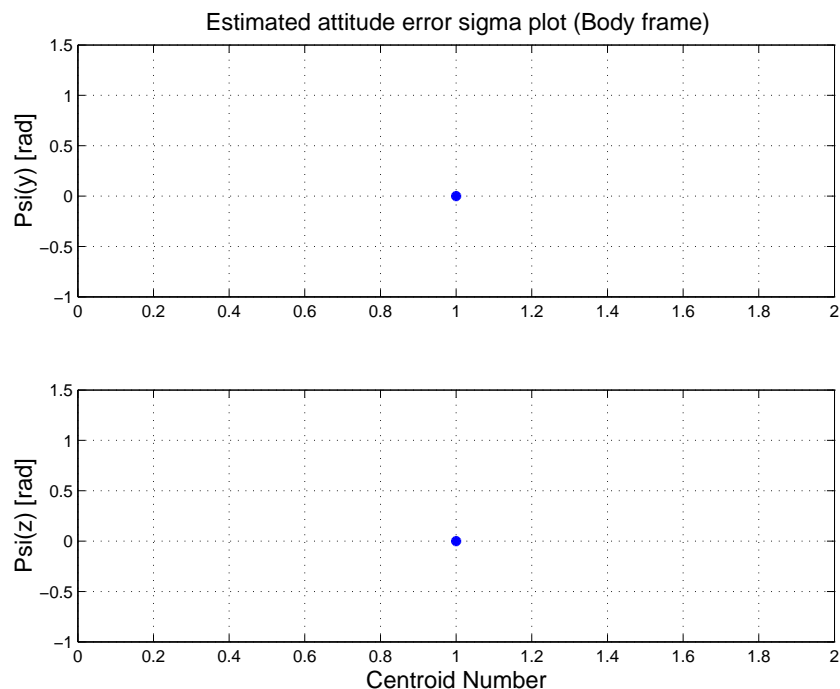


Figure 3.34: Estimated attitude error sigma plot (Body frame)

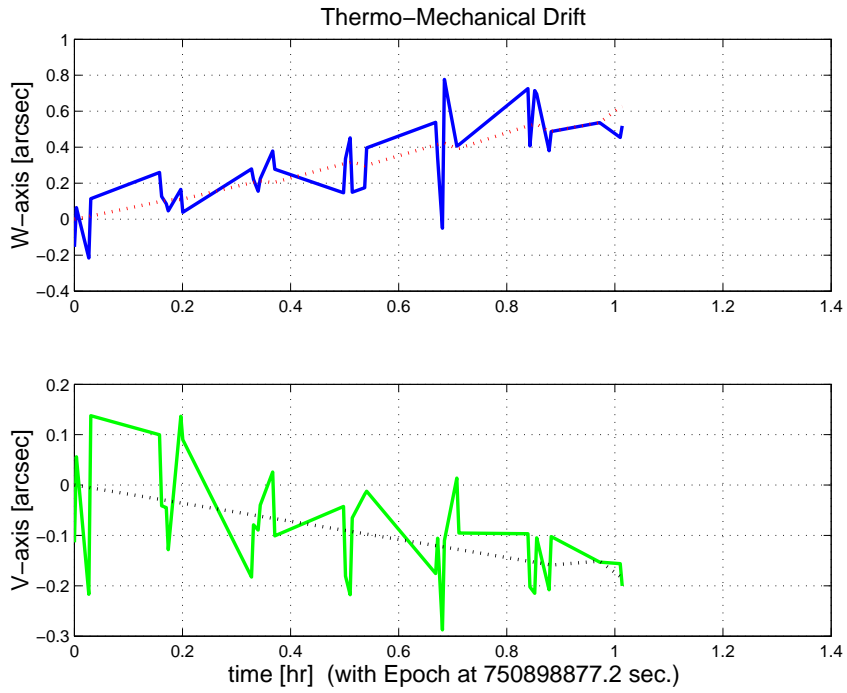


Figure 3.35: Thermo-mechanical boresight drift (equiv. angle in (W,V) coords)

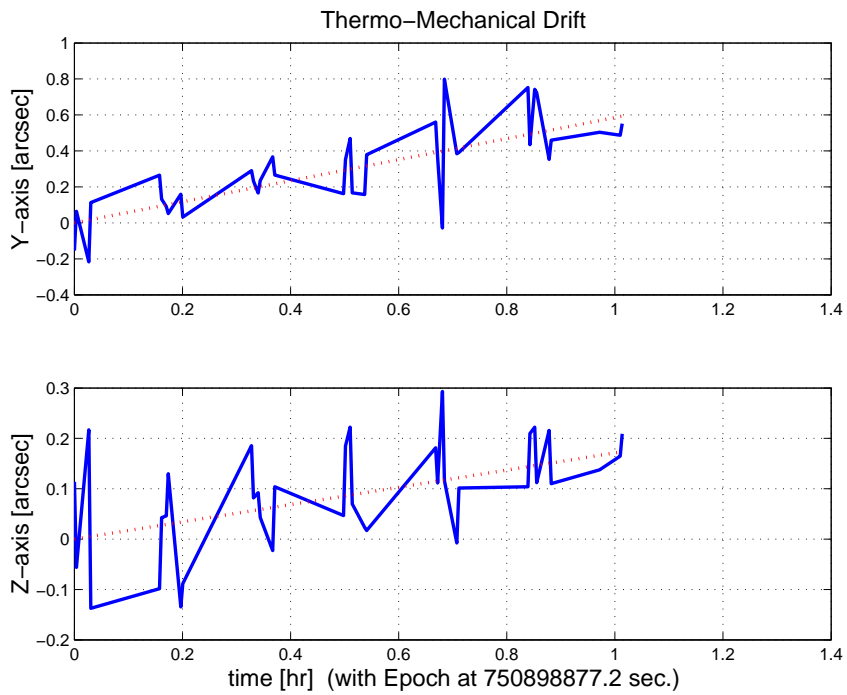


Figure 3.36: Thermo-mechanical boresight drift (equiv. angle in Body frame)

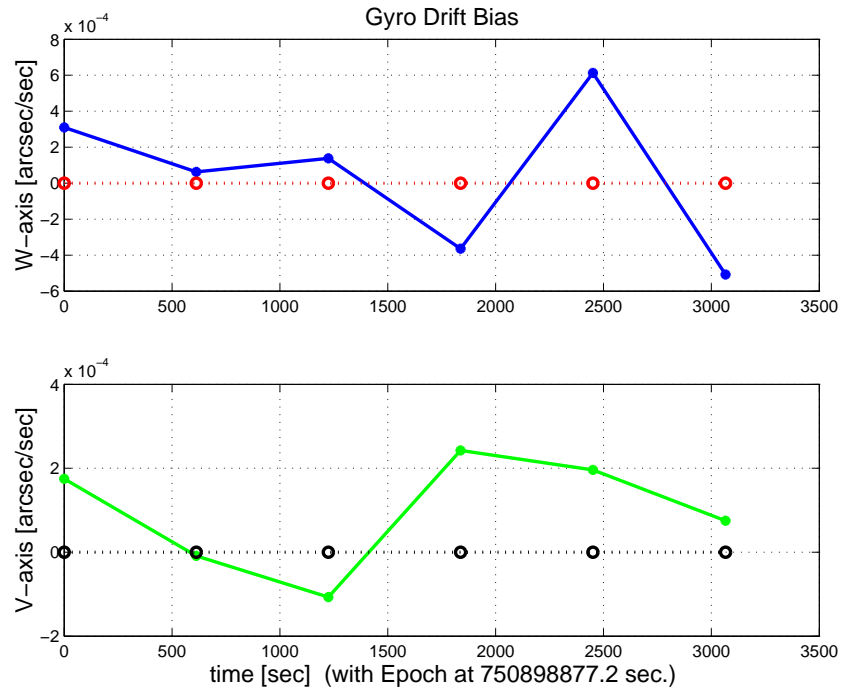


Figure 3.37: Gyro drift bias contribution (equiv. rate in (W,V) coords)

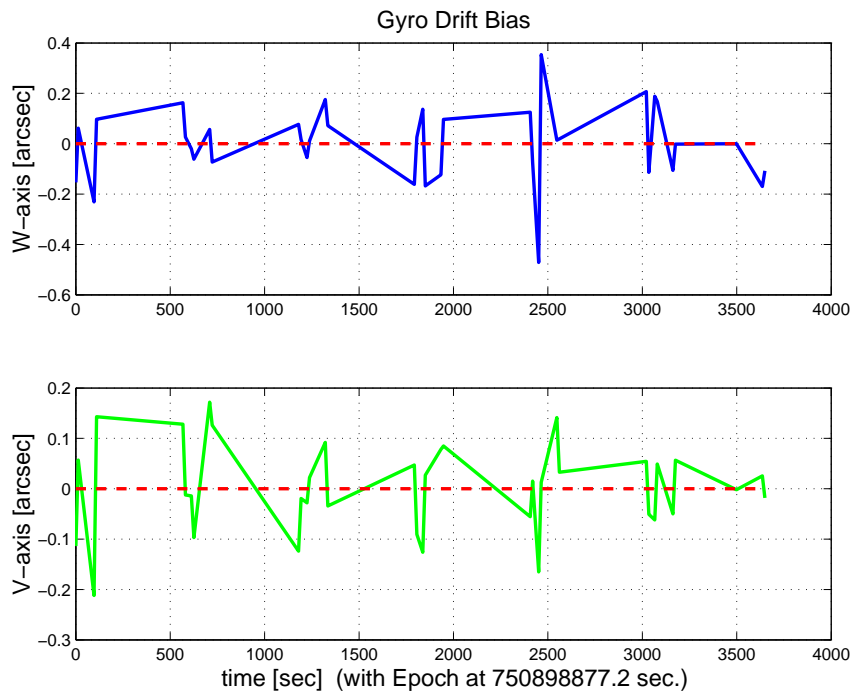


Figure 3.38: Gyro drift bias contribution (equiv. angle in (W,V) coords)

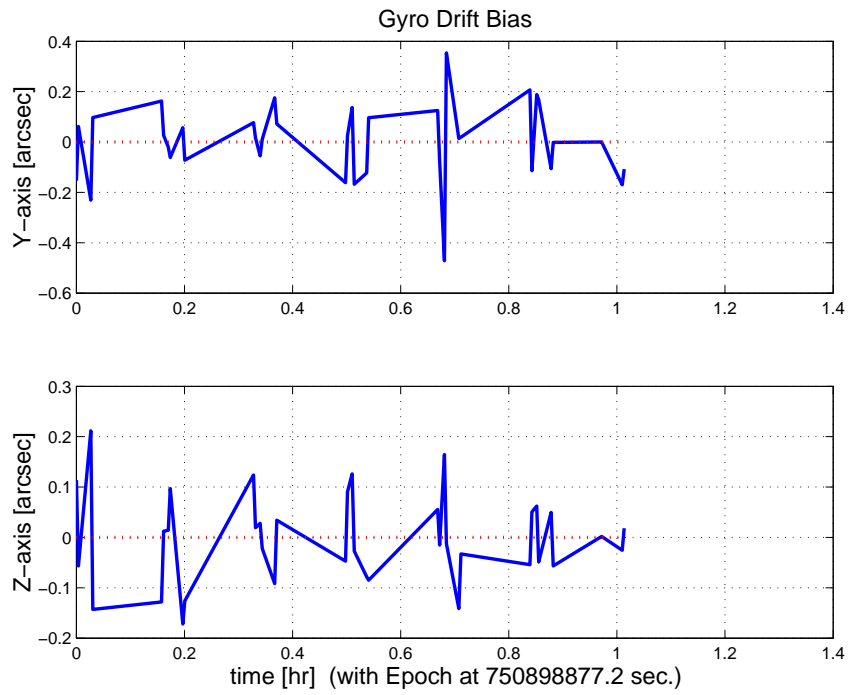


Figure 3.39: Gyro drift bias contribution (equiv. angle in Body frame)

3.2 IPF OUTPUT DATA (IF MINI FILE)

OUTPUT FILE NAME: IFmini002121.dat DATE: 20-Oct-2003 TIME: 18:17
 INSTRUMENT NAME: MIPS_SED_center NF: 121
 IPF FILTER VERSION: IPF.V2.0.0C SW RELEASE DATE: August 1, 2003
 FRAME TABLE USED: BodyFrames_SPC_08a

----- IPF BROWN ANGLE SUMMARY -----						
Frame Number	WAS			IS		
	theta_Y (arcmin)	theta_Z (arcmin)	angle (deg)	theta_Y (arcmin)	theta_Z (arcmin)	angle (deg)
121	+6.073000	-11.098000	-0.000000	+6.099911	-9.595594	+0.000044
113	+6.830000	-12.398000	+0.000000	+6.758890	-11.007261	+0.000044
114	+5.479000	-12.391000	+0.000000	+5.440933	-11.007261	+0.000044
116	+6.723000	-10.701000	-0.000000	+6.758889	-9.102260	+0.000044
117	+5.373000	-10.695000	+0.000000	+5.440932	-9.102261	+0.000044
122	+6.781000	-11.623000	+0.000000	+6.758890	-10.077261	+0.000044
123	+5.430000	-11.616000	+0.000000	+5.440933	-10.077261	+0.000044
125	+6.802000	-11.957000	-0.000000	+6.758890	-10.548928	+0.000044
126	+5.451000	-11.951000	-0.000000	+5.440933	-10.548928	+0.000044
<hr/>						
OFFSET	NF	Delta_CW	Delta_CV			
0	121	+0.000	+0.000	pixels		
OFFSET FRAME NAME: MIPS_SED_center						
Brown Angle	theta_Y(arcmin)	theta_Z(arcmin)	angle(deg)			
WAS(FTB)	+6.073000	-11.098000	-0.000000			
IS (EST)	+6.099911	-9.595594	+0.000044			
dT_EST	+0.026911	+1.502406	+0.000044			
T_sSIGMA	+0.221501	+0.380933	+999.999999			
dT_EST/T_sSIGMA	+0.121493	+3.944014	+999.999999			
<hr/>						
OFFSET	NF	Delta_CW	Delta_CV			
1	113	+4.000	+8.470	pixels		
OFFSET FRAME NAME: MIPS_SED_5						
Brown Angle	theta_Y(arcmin)	theta_Z(arcmin)	angle(deg)			
WAS(FTB)	+6.830000	-12.398000	+0.000000			
IS (EST)	+6.758890	-11.007261	+0.000044			
dT_EST	-0.071110	+1.390739	+0.000044			
T_sSIGMA	+0.221501	+0.380933	+999.999999			
dT_EST/T_sSIGMA	-0.321037	+3.650872	+999.999999			
<hr/>						
OFFSET	NF	Delta_CW	Delta_CV			
2	114	-4.000	+8.470	pixels		
OFFSET FRAME NAME: MIPS_SED_6						
Brown Angle	theta_Y(arcmin)	theta_Z(arcmin)	angle(deg)			
WAS(FTB)	+5.479000	-12.391000	+0.000000			
IS (EST)	+5.440933	-11.007261	+0.000044			
dT_EST	-0.038067	+1.383739	+0.000044			
T_sSIGMA	+0.221501	+0.380933	+999.999999			
dT_EST/T_sSIGMA	-0.171859	+3.632496	+999.999999			
<hr/>						
OFFSET	NF	Delta_CW	Delta_CV			
3	116	+4.000	-2.960	pixels		
OFFSET FRAME NAME: MIPS_SED_7						
Brown Angle	theta_Y(arcmin)	theta_Z(arcmin)	angle(deg)			
WAS(FTB)	+6.723000	-10.701000	-0.000000			
IS (EST)	+6.758889	-9.102260	+0.000044			
dT_EST	+0.035889	+1.598740	+0.000044			
T_sSIGMA	+0.221501	+0.380933	+999.999999			
dT_EST/T_sSIGMA	+0.162026	+4.196904	+999.999999			
<hr/>						
OFFSET	NF	Delta_CW	Delta_CV			
4	117	-4.000	-2.960	pixels		
OFFSET FRAME NAME: MIPS_SED_8						

Brown Angle	theta_Y(arcmin)	theta_Z(arcmin)	angle(deg)	
WAS(FTB)	+5.373000	-10.695000	+0.000000	
IS (EST)	+5.440932	-9.102261	+0.000044	
dT_EST	+0.067932	+1.592739	+0.000044	
T_sSIGMA	+0.221501	+0.380933	+999.999999	
dT_EST/T_sSIGMA	+0.306689	+4.181150	+999.999999	

OFFSET	NF	Delta_CW	Delta_CV	
5	122	+4.000	+2.890	pixels

OFFSET FRAME NAME: MIPS_SED_1

Brown Angle	theta_Y(arcmin)	theta_Z(arcmin)	angle(deg)	
WAS(FTB)	+6.781000	-11.623000	+0.000000	
IS (EST)	+6.758890	-10.077261	+0.000044	
dT_EST	-0.022110	+1.545739	+0.000044	
T_sSIGMA	+0.221501	+0.380933	+999.999999	
dT_EST/T_sSIGMA	-0.099820	+4.057770	+999.999999	

OFFSET	NF	Delta_CW	Delta_CV	
6	123	-4.000	+2.890	pixels

OFFSET FRAME NAME: MIPS_SED_2

Brown Angle	theta_Y(arcmin)	theta_Z(arcmin)	angle(deg)	
WAS(FTB)	+5.430000	-11.616000	+0.000000	
IS (EST)	+5.440933	-10.077261	+0.000044	
dT_EST	+0.010933	+1.538739	+0.000044	
T_sSIGMA	+0.221501	+0.380933	+999.999999	
dT_EST/T_sSIGMA	+0.049358	+4.039392	+999.999999	

OFFSET	NF	Delta_CW	Delta_CV	
7	125	+4.000	+5.720	pixels

OFFSET FRAME NAME: MIPS_SED_3

Brown Angle	theta_Y(arcmin)	theta_Z(arcmin)	angle(deg)	
WAS(FTB)	+6.802000	-11.957000	-0.000000	
IS (EST)	+6.758890	-10.548928	+0.000044	
dT_EST	-0.043110	+1.408072	+0.000044	
T_sSIGMA	+0.221501	+0.380933	+999.999999	
dT_EST/T_sSIGMA	-0.194627	+3.696376	+999.999999	

OFFSET	NF	Delta_CW	Delta_CV	
8	126	-4.000	+5.720	pixels

OFFSET FRAME NAME: MIPS_SED_4

Brown Angle	theta_Y(arcmin)	theta_Z(arcmin)	angle(deg)	
WAS(FTB)	+5.451000	-11.951000	-0.000000	
IS (EST)	+5.440933	-10.548928	+0.000044	
dT_EST	-0.010067	+1.402072	+0.000044	
T_sSIGMA	+0.221501	+0.380933	+999.999999	
dT_EST/T_sSIGMA	-0.045449	+3.680624	+999.999999	

VARNAME	MEAN	SIGMA	SCALED_SIGMA
del_theta2	+2.2952125158179746E-018	+4.7923432184008452E-005	+6.4432074831706894E-005
del_theta3	-1.3989119700819194E-017	+8.2417758559929640E-005	+1.1080899144713065E-004
del_arx	+2.0629131676540638E-015	+6.2256715544554796E-005	+8.3702881282396620E-005
del_ary	-1.6871837518121598E-018	+2.0595314542211318E-006	+2.7689979354381603E-006
del_arz	+7.6673819432153292E-018	+2.0321678082976591E-006	+2.7322080729124573E-006
brx	+1.5292377932832799E-008	+3.1609742676141092E-008	+4.2498652803079935E-008
bry	+7.8873556758549518E-010	+3.4388457174818134E-010	+4.6234577638915276E-010
brz	+2.3072374757047450E-010	+2.7612049489706979E-010	+3.7123836042178589E-010

LSQF RESIDUAL SIGMA SCALE = +1.3444795561451295E+000

qT	qT(1)	qT(2)	qT(3)	qT(4)
FrmTbl:	+1.4257389017362338E-006	-8.8328078008885079E-004	+1.6141373392967960E-003	+9.9999830718540750E-001
Estim:	+1.6250689842247365E-006	-8.8719456244559217E-004	+1.3956219077790740E-003	+9.9999863256039412E-001
DelTheta	deltheta(1)	deltheta(2)	deltheta(3)	[rad]
	+1.7134307175740354E-009	-7.8282430645880156E-006	-4.3703151807988400E-004	

EulAngT	theta(1)	theta(2)	theta(3)	[rad]
Mean	+7.7375840653539195E-007	-1.7743921655875188E-003	+2.7912451337149613E-003	
SigmaT	+9.9999000000000000E+004	+4.7923432184008452E-005	+8.2417758559929640E-005	
<hr/>				
qR	qR(1)	qR(2)	qR(3)	qR(4)
ASFILE:	+7.0019613485783339E-004	+1.2696074554696679E-003	-1.613295890056068E-004	+9.9999892711639404E-001
Estim:	+4.8627393122513797E-004	+1.2688277990249690E-003	-1.6070659123726245E-004	+9.9999906389309767E-001
DelThetaR	delthetaR(1)	delthetaR(2)	delthetaR(3)	
	-4.2784547773666636E-004	-1.6276594309438210E-006	+7.0428571331547734E-007	[rad]
EulAngR	angR(1)	angR(2)	angR(3)	[rad]
Mean	+9.7214241771795967E-004	+2.5378122415100680E-003	-3.2017992236159647E-004	
SigmaR	+6.2256715544554796E-005	+2.0595314542211318E-006	+2.0321678082976591E-006	
<hr/>				
Initial Gyro Bias	Bg0(1)	Bg0(2)	Bg0(3)	
	+0.0000000000000000E+000	+0.0000000000000000E+000	+0.0000000000000000E+000	
Gyro Bias Correction	Bg(1)	Bg(2)	Bg(3)	
	+0.0000000000000000E+000	+0.0000000000000000E+000	+0.0000000000000000E+000	
Total Gyro Bias	BgT(1)	BgT(2)	BgT(3)	
	+0.0000000000000000E+000	+0.0000000000000000E+000	+0.0000000000000000E+000	
Initial Gyro Bias Rate	Cg0(1)	Cg0(2)	Cg0(3)	
	+0.0000000000000000E+000	+0.0000000000000000E+000	+0.0000000000000000E+000	
Gyro Bias Rate Correction	Cg(1)	Cg(2)	Cg(3)	
	+0.0000000000000000E+000	+0.0000000000000000E+000	+0.0000000000000000E+000	
Total Gyro Bias Rate	CgT(1)	CgT(2)	CgT(3)	
	+0.0000000000000000E+000	+0.0000000000000000E+000	+0.0000000000000000E+000	
<hr/>				
OFFSET	NF	Delta_CW	Delta_CV	
1	113	+4.000	+8.470	pixels
OFFSET FRAME NAME: MIPS_SED_5				
qT	qT(1)	qT(2)	qT(3)	qT(4)
WAS(FTB)	+1.7912832792639671E-006	-9.9338145417754453E-004	+1.8032141385842637E-003	+9.9999788080217855E-001
IS (EST)	+1.9606680113611594E-006	-9.830386529322531E-004	+1.6009401981930285E-003	+9.9999823530926513E-001
DelTheta	deltheta(1)	deltheta(2)	deltheta(3)	
Units	rad	rad	rad	
	-2.9986344467597569E-008	+2.0684921799604875E-005	-4.0454867864138887E-004	
EulAngT	theta(1)	theta(2)	theta(3)	[rad]
Mean	+7.7375840653539206E-007	-1.9660813808103335E-003	+3.2018825505948680E-003	
sSigmaT	+3.3929342009685447E-008	+6.4432069398702817E-005	+1.1080898941173252E-004	
SigmaT	+2.5236041600340224E-008	+4.7923428143036576E-005	+8.2417757046036679E-005	
<hr/>				
OFFSET	NF	Delta_CW	Delta_CV	
2	114	-4.000	+8.470	pixels
OFFSET FRAME NAME: MIPS_SED_6				
qT	qT(1)	qT(2)	qT(3)	qT(4)
WAS(FTB)	+1.4361493944558119E-006	-7.9688686918524690E-004	+1.8021963489983767E-003	+9.9999805852690271E-001
IS (EST)	+1.6537854288286519E-006	-7.9134992722646358E-004	+1.6009404049481684E-003	+9.9999840537491735E-001
DelTheta	deltheta(1)	deltheta(2)	deltheta(3)	
Units	rad	rad	rad	
	+1.3224257727695262E-007	+1.1073079541207466E-005	-4.0251272156845483E-004	
EulAngT	theta(1)	theta(2)	theta(3)	[rad]
Mean	+7.7375840653539195E-007	-1.5827032866291386E-003	+3.2018825678955649E-003	
sSigmaT	+3.3929622285454178E-008	+6.4432069398710217E-005	+1.1080898941164239E-004	
SigmaT	+2.5236250064475994E-008	+4.7923428143042072E-005	+8.2417757045969648E-005	
<hr/>				
OFFSET	NF	Delta_CW	Delta_CV	
3	116	+4.000	-2.960	pixels
OFFSET FRAME NAME: MIPS_SED_7				
qT	qT(1)	qT(2)	qT(3)	qT(4)
WAS(FTB)	+1.5218767204458424E-006	-9.7781937328597114E-004	+1.5563959880422460E-003	+9.9999831074781598E-001
IS (EST)	+1.6882959773091455E-006	-9.8303901681744610E-004	+1.3238693523596624E-003	+9.9999864049976539E-001
DelTheta	deltheta(1)	deltheta(2)	deltheta(3)	

```

Units           rad           rad           rad
              -1.3572126518103634E-007 -1.0439882176076785E-005 -4.6505382527946813E-004
EulAngT        theta(1)      theta(2)      theta(3)          [rad]
Mean          +7.7375840653539195E-007 -1.9660810975572198E-003 +2.6477399968493085E-003
sSigmaT        +2.3166184871098887E-008 +6.4432074168504979E-005 +1.1080898941115339E-004
SigmaT         +1.7230596601647560E-008 +4.7923431690730656E-005 +8.2417757045605939E-005
-----

OFFSET        NF       Delta_CW       Delta_CV
4            117      -4.000      -2.960      pixels
OFFSET FRAME NAME: MIPS_SED_8
qT            qT(1)      qT(2)      qT(3)      qT(4)
WAS(FTB)     +1.2155970940874027E-006 -7.8147014759424752E-004 +1.5555235935568977E-003 +9.9999848482349241E-001
IS (EST)    +1.4345249762421944E-006 -7.9135019925322093E-004 +1.3238697004757565E-003 +9.9999881056520268E-001

DelTheta      deltheta(1)      deltheta(2)      deltheta(3)
Units         rad           rad           rad
              +4.9633471234176525E-008 -1.9760797586365406E-005 -4.6330842037474337E-004
EulAngT        theta(1)      theta(2)      theta(3)          [rad]
Mean          +7.7375840653539195E-007 -1.5827029750006950E-003 +2.6477403911130460E-003
sSigmaT        +2.3166041415343837E-008 +6.4432074168505873E-005 +1.1080898941118285E-004
SigmaT         +1.7230489901806425E-008 +4.7923431690731320E-005 +8.2417757045627854E-005
-----

OFFSET        NF       Delta_CW       Delta_CV
5            122      +4.000      +2.890      pixels
OFFSET FRAME NAME: MIPS_SED_1
qT            qT(1)      qT(2)      qT(3)      qT(4)
WAS(FTB)     +1.6672623689367301E-006 -9.8625490234101874E-004 +1.6904951973088730E-003 +9.9999808476040375E-001
IS (EST)    +1.8276990549600744E-006 -9.8303887771708661E-004 +1.4656772848250000E-003 +9.9999844270944782E-001

DelTheta      deltheta(1)      deltheta(2)      deltheta(3)
Units         rad           rad           rad
              -1.1315652908973831E-007 +6.4314256140531216E-006 -4.4963650537042536E-004
EulAngT        theta(1)      theta(2)      theta(3)          [rad]
Mean          +7.7375840653539206E-007 -1.9660813179535352E-003 +2.9313562749295930E-003
sSigmaT        +2.3079638725387104E-008 +6.4432074199041086E-005 +1.1080898941145747E-004
SigmaT         +1.7166225116550435E-008 +4.7923431713442869E-005 +8.2417757045832104E-005
-----

OFFSET        NF       Delta_CW       Delta_CV
6            123      -4.000      +2.890      pixels
OFFSET FRAME NAME: MIPS_SED_2
qT            qT(1)      qT(2)      qT(3)      qT(4)
WAS(FTB)     +1.3342844486955502E-006 -7.8976027730581907E-004 +1.6894773853233871E-003 +9.9999826097003219E-001
IS (EST)    +1.5467449455678850E-006 -7.9135009797488571E-004 +1.4656775605910004E-003 +9.9999861277499702E-001

DelTheta      deltheta(1)      deltheta(2)      deltheta(3)
Units         rad           rad           rad
              +6.6762731985029044E-008 -3.1803803832655425E-006 -4.4760039499499985E-004
EulAngT        theta(1)      theta(2)      theta(3)          [rad]
Mean          +7.7375840653539206E-007 -1.5827031952123597E-003 +2.9313564762594923E-003
sSigmaT        +2.3079779312965917E-008 +6.4432074199041966E-005 +1.1080898941142768E-004
SigmaT         +1.7166329683093057E-008 +4.7923431713443519E-005 +8.2417757045809945E-005
-----

OFFSET        NF       Delta_CW       Delta_CV
7            125      +4.000      +5.720      pixels
OFFSET FRAME NAME: MIPS_SED_3
qT            qT(1)      qT(2)      qT(3)      qT(4)
WAS(FTB)     +1.7204846814229829E-006 -9.8930914026667638E-004 +1.7390734278563290E-003 +9.9999799844203563E-001
IS (EST)    +1.8951367351895431E-006 -9.8303877495208177E-004 +1.5342783741593663E-003 +9.9999833980914499E-001

DelTheta      deltheta(1)      deltheta(2)      deltheta(3)
Units         rad           rad           rad
              -3.6667899815132706E-008 +1.2540061558032042E-005 -4.0959084514748269E-004
EulAngT        theta(1)      theta(2)      theta(3)          [rad]
Mean          +7.7375840653539195E-007 -1.9660813678146062E-003 +3.0685586742676563E-003

```

```

sSigmaT +2.7756596496747814E-008 +6.4432072353762544E-005 +1.1080898941159879E-004
SigmaT +2.0644863188794843E-008 +4.7923430340957478E-005 +8.2417757045937217E-005
-----

OFFSET          NF        Delta_CW        Delta_CV
    8           126       -4.000       +5.720      pixels
OFFSET FRAME NAME: MIPS_SED_4
qT             qT(1)            qT(2)            qT(3)            qT(4)
WAS(FTB) +1.3780735821712564E-006 -7.9281453197768193E-004 +1.7382010693171191E-003 +9.9999817504846544E-001
IS (EST) +1.6010325177073825E-006 -7.9135002042393513E-004 +1.5342786149252325E-003 +9.9999850987474659E-001

DelTheta      deltheta(1)      deltheta(2)      deltheta(3)
Units         rad             rad             rad
+1.2706486320823944E-007 +2.9282375095503061E-006 -4.0784568868503684E-004
EulAngT       theta(1)        theta(2)        theta(3)        [rad]
Mean          +7.7375840653539195E-007 -1.5827032560517093E-003 +3.0685587822637428E-003
sSigmaT       +2.7756827866946652E-008 +6.4432072353765919E-005 +1.1080898941153886E-004
SigmaT       +2.0645035277836867E-008 +4.7923430340959985E-005 +8.2417757045892643E-005
-----

q(1)          q(2)          q(3)          q(4)
PCRS1A: +5.3377191730804340E-007 +3.7444181445836429E-004 -1.4255121007937610E-003 +9.9999891385355677E-001
PCRS2A: -5.2784857378083422E-007 +3.8463011681657313E-004 +1.3723523317471205E-003 +9.9999898435372037E-001
-----
```

***** CS-FILE PARAMETERS: ***** AS-FILE PARAMETERS: *****

```

Row (01) PIX2RADX: +4.792226640000000E-005 Row (1) TASTART: +7.5089800029074097E+008
Row (02) PIX2RADY: +4.8481322570479732E-005 Row (2) TASTOP: +7.5090300019078672E+008
Row (03) CX0: +1.250000000000000E+001 Row (3) S/C TIME: +7.5088810549076843E+008
Row (04) CY0: +1.500000000000000E+000 Row (4) QR1: +7.0019613485783339E-004
Row (05) BETA0: +2.8047410000000001E-006 Row (5) QR2: +1.2696074554696679E-003
Row (06) GAMMA_E0: +3.220000000000000E+003 Row (6) QR3: -1.6132958990056068E-004
Row (07) D11: +1.000000000000000E+000 Row (7) QR4: +9.9999892711639404E-001
Row (08) D12: +0.000000000000000E+000
Row (09) D21: +0.000000000000000E+000
Row (10) D22: -1.000000000000000E+000
Row (11) DG: -1.000000000000000E+000
-----
```

INITIAL STA-TO-PCRS ALIGNMENT (R) KNOWLEDGE (1-SIGMA)

```

SIGMA(X) SIGMA(Y) SIGMA(Z)
1.03875511E+001 3.90072739E-001 3.90593874E-001 [arcsec]
-----
```

```

PIX2RADX = 4.792226640000E-005[rad/pixel]
XPIXSIZEx = 9.8847[arcsec]
PIX2RADY = 4.848132257048E-005[rad/pixel]
YPIXSIZEx = 10.0000[arcsec]
CX0 = 12.5[pixel] = 123.56[arcsec]
CY0 = 1.5[pixel] = 15.00[arcsec]
-----
```

```

NOMINAL BETA0 = 2.804741000000E-006[rad/encoder unit]
ENCODER UNIT SIZE = 0.58[arcsec]
GAMMA_E0 = 3220.00[encoder unit] = 1862.83[arcsec]
-----
```

```

FLIP MATRIX D = | +1 | +0 |
                  | --- | --- |   and   DG = -1
                  | +0 | -1 |
-----
```

3.3 IPF EXECUTION LOG

```
*****
IPF EXECUTION-LOG FILE NAME: LG002121.dat
INSTRUMENT TYPE: MIPS_SED_center
IPF FILTER EXECUTION DATE: 20-Oct-2003 TIME: 18:16
IPF FILTER VERSION USED: IPF.V2.0.0C
*****
```

```
*****
SLIT FLAG ENABLED! ENTERING SLIT MODE.
*****
```

```
----- Loading & Preparing Input Files -----
AAFILE: AA001121 Loaded! AAFILE dimension = 50000 X 21
ASFILE: AS001121 Loaded!
CAFILe: CA002121 Loaded! CAFILe dimension = 1 X 15
CBFILE: CB002121 Loaded! CBFILE dimension = 36 X 15
CCFILE: CC002121 Created! CCFILE dimension = 37 X 19
CSFILE: CS002121 Loaded!
Loading Input Files Completed!
```

```
----- Selected Mask Vectors -----
index = 1 2 3 4 5 6 7 8 9 10 11 12 13 14 15 16 17 18 19 20
```

```
----- mask1 = [ 0 0 0 0 0 0 0 0 0 0 0 0 0 0 0 0 0 0 0 0 ]  

mask2 = [ 0 0 0 1 1 1 1 1 1 0 0 0 0 0 0 0 0 0 0 0 ]
```

```
----- Selected Initial Gyro Bias Parameters -----
IPF Filter in LITE MODE# 2
IPF LITE MODE WITH UNFILTERED STA QUATERNION!
IPF Linearized Using Following Nominal Gyro Bias Estimates
bg0 = [+0.00000000000000E+000 +0.00000000000000E+000 +0.00000000000000E+000 ]
cg0 = [+0.00000000000000E+000 +0.00000000000000E+000 +0.00000000000000E+000 ]
```

```
----- Gyro Pre-Processor Run Completed -----
AGFILE CREATED: AG002121.m ACFILE CREATED: AC002121.m
```

```
Total Gyro Preprocessor Execution Time: 0 seconds
```

```
FRAME TABLE ENTRIES FOR PCRS LOADED TO TPCRS
q_PCRS4 = [ +5.3377191730804340E-007 q_PCRS5 = [ +7.3379987833742897E-007  

+3.7444181445836429E-004 +5.2236196154513707E-004  

-1.4255121007937610E-003 -1.4047712280184723E-003  

+9.9999891385355677E-001 ]; +9.9999887687698918E-001 ];  

q_PCRS8 = [ -5.2784857378083422E-007 q_PCRS9 = [ -7.1963421681856818E-007  

+3.8463011681657313E-004 +5.3239763239987400E-004  

+1.3723523317471205E-003 +1.3516841804518383E-003  

+9.9999898435372037E-001 ]; +9.9999894475050310E-001 ];
```

```
----- Initial Conditions for State ----- ----- Initial Square-Root Cov (diag) -----  

p1(01) = a00 = +0.0000000000000000E+000 Sigma_initial(01,01) = 9.9999000000000000E+004  

p1(02) = b00 = +0.0000000000000000E+000 Sigma_initial(02,02) = 9.9999000000000000E+004  

p1(03) = c00 = +0.0000000000000000E+000 Sigma_initial(03,03) = 9.9999000000000000E+004  

p1(04) = a10 = +0.0000000000000000E+000 Sigma_initial(04,04) = 9.9999000000000000E+004  

p1(05) = b10 = +0.0000000000000000E+000 Sigma_initial(05,05) = 9.9999000000000000E+004  

p1(06) = c10 = +0.0000000000000000E+000 Sigma_initial(06,06) = 9.9999000000000000E+004  

p1(07) = d10 = +0.0000000000000000E+000 Sigma_initial(07,07) = 9.9999000000000000E+004  

p1(08) = a20 = +0.0000000000000000E+000 Sigma_initial(08,08) = 9.9999000000000000E+004  

p1(09) = b20 = +0.0000000000000000E+000 Sigma_initial(09,09) = 9.9999000000000000E+004  

p1(10) = c20 = +0.0000000000000000E+000 Sigma_initial(10,10) = 9.9999000000000000E+004  

p1(11) = d20 = +0.0000000000000000E+000 Sigma_initial(11,11) = 9.9999000000000000E+004  

p1(12) = a01 = +0.0000000000000000E+000 Sigma_initial(12,12) = 9.9999000000000000E+004  

p1(13) = b01 = +0.0000000000000000E+000 Sigma_initial(13,13) = 9.9999000000000000E+004  

p1(14) = c01 = +0.0000000000000000E+000 Sigma_initial(14,14) = 9.9999000000000000E+004  

p1(15) = d01 = +0.0000000000000000E+000 Sigma_initial(15,15) = 9.9999000000000000E+004
```

```

p1(16) = e01 = +0.0000000000000000E+000 Sigma_initial(16,16) = 9.9999000000000000E+004
p1(17) = f01 = +0.0000000000000000E+000 Sigma_initial(17,17) = 9.9999000000000000E+004
-----
p2f(01) = am1 = +0.0000000000000000E+000 Sigma_initial(18,18) = 9.9999000000000000E+004
p2f(02) = am2 = +0.0000000000000000E+000 Sigma_initial(19,19) = 9.9999000000000000E+004
p2f(03) = am3 = +1.0000000000000000E+000 Sigma_initial(20,20) = 9.9999000000000000E+004
p2f(04) = beta = +1.0000000000000000E+000 Sigma_initial(21,21) = 1.0000000000000000E-002
p2f(05) = qT1 = +1.4257389017362338E-006 Sigma_initial(22,22) = 1.0000000000000000E-002
p2f(06) = qT2 = -8.832807800885079E-004 Sigma_initial(23,23) = 5.0360268829562863E-004
p2f(07) = aT3 = +1.6141373392967960E-003 Sigma_initial(24,24) = 1.8911260069207081E-005
p2f(08) = qT4 = +9.9999830718540750E-001 Sigma_initial(25,25) = 1.8936525388250984E-005
p2f(09) = qR1 = +7.0019613485783339E-004 Sigma_initial(26,26) = 2.7404768658900291E-004
p2f(10) = qR2 = +1.2696074554696679E-003 Sigma_initial(27,27) = 2.7404768658900291E-004
p2f(11) = qR3 = -1.6132958990056068E-004 Sigma_initial(28,28) = 2.7404768658900291E-004
p2f(12) = qR4 = +9.9999892711639404E-001 Sigma_initial(29,29) = 9.9999000000000000E+004
p2f(13) = brx = +0.0000000000000000E+000 Sigma_initial(30,30) = 9.9999000000000000E+004
p2f(14) = bry = +0.0000000000000000E+000 Sigma_initial(31,31) = 9.9999000000000000E+004
p2f(15) = brz = +0.0000000000000000E+000 Sigma_initial(32,32) = 9.9999000000000000E+004
p2f(16) = crx = +0.0000000000000000E+000 Sigma_initial(33,33) = 9.9999000000000000E+004
p2f(17) = cry = +0.0000000000000000E+000 Sigma_initial(34,34) = 9.9999000000000000E+004
p2f(18) = crz = +0.0000000000000000E+000 Sigma_initial(35,35) = 9.9999000000000000E+004
p2f(19) = bgx = +0.0000000000000000E+000 Sigma_initial(36,36) = 9.9999000000000000E+004
p2f(20) = bgy = +0.0000000000000000E+000 Sigma_initial(37,37) = 9.9999000000000000E+004
p2f(21) = bgz = +0.0000000000000000E+000
p2f(22) = cgx = +0.0000000000000000E+000
p2f(23) = cgy = +0.0000000000000000E+000
p2f(24) = cgz = +0.0000000000000000E+000
-----
```

```

----- IPF KALMAN FILTER STARTED -----
Iteration#001: |dp|= +6.072265952138E-004 RMS(|Res|)=+4.352789139141E-004
Iteration#002: |dp|= +1.264308193286E-005 RMS(|Res|)=+9.976350962244E-007
Iteration#003: |dp|= +6.017456391782E-006 RMS(|Res|)=+9.623548279369E-007
Iteration#004: |dp|= +3.920852040075E-007 RMS(|Res|)=+9.727761668989E-007
Iteration#005: |dp|= +7.8977991191156E-008 RMS(|Res|)=+9.731050645334E-007
Iteration#006: |dp|= +8.608358308742E-009 RMS(|Res|)=+9.730403171677E-007
Iteration#007: |dp|= +9.226316834823E-010 RMS(|Res|)=+9.730406188364E-007
Iteration#008: |dp|= +1.622449582609E-010 RMS(|Res|)=+9.730408098546E-007
Iteration#009: |dp|= +8.738801915452E-012 RMS(|Res|)=+9.730407020797E-007
Iteration#010: |dp|= +2.768147554611E-012 RMS(|Res|)=+9.730407022112E-007
Iteration#011: |dp|= +3.551769683619E-014 RMS(|Res|)=+9.730407053984E-007
Iteration#012: |dp|= +4.371280578234E-014 RMS(|Res|)=+9.730407055540E-007
Iteration#013: |dp|= +5.277320060974E-015 RMS(|Res|)=+9.730407053997E-007
Iteration#014: |dp|= +2.274783261851E-015 RMS(|Res|)=+9.730407053792E-007
Iteration#015: |dp|= +2.148985492892E-015 RMS(|Res|)=+9.730407053997E-007
Iteration#016: |dp|= +1.643763623070E-015 RMS(|Res|)=+9.730407053933E-007
Iteration#017: |dp|= +2.223135483860E-015 RMS(|Res|)=+9.730407054062E-007
Iteration#018: |dp|= +2.581298855454E-015 RMS(|Res|)=+9.730407054139E-007
Iteration#019: |dp|= +1.545791381986E-015 RMS(|Res|)=+9.730407053663E-007
Iteration#020: |dp|= +1.590781057769E-015 RMS(|Res|)=+9.730407054126E-007
Iteration#021: |dp|= +2.362528961289E-016 RMS(|Res|)=+9.730407054807E-007
Iteration#022: |dp|= +4.586005230443E-015 RMS(|Res|)=+9.730407053997E-007
Iteration#023: |dp|= +9.973750324211E-016 RMS(|Res|)=+9.730407054396E-007
Iteration#024: |dp|= +3.016691438649E-015 RMS(|Res|)=+9.730407053933E-007
Iteration#025: |dp|= +2.062976816638E-015 RMS(|Res|)=+9.730407054061E-007
IPF Kalman Filter Completed with Error |dp1| + |dp2| = +2.0629768166377001E-015
-----
```

```

----- IPF LEAST SQUARES FILTER STARTED -----
Iteration#001 COND#=+1.323328197640E+002, |dp|=+6.117980764913E-004
Iteration#002 COND#=+1.323307505219E+002, |dp|=+4.907954176663E-008
Iteration#003 COND#=+1.323307482480E+002, |dp|=+2.681532776877E-012
Iteration#004 COND#=+1.323307482483E+002, |dp|=+2.338200844200E-015
Iteration#005 COND#=+1.323307482483E+002, |dp|=+3.030291726427E-015
Iteration#006 COND#=+1.323307482483E+002, |dp|=+1.463262930253E-015
Iteration#007 COND#=+1.323307482483E+002, |dp|=+5.715311074527E-015
Iteration#008 COND#=+1.323307482483E+002, |dp|=+1.976095647214E-015
Iteration#009 COND#=+1.323307482483E+002, |dp|=+2.427638553519E-015
-----
```

```

Iteration#010 COND#=+1.323307482483E+002, |dp|=+2.555567521364E-015
Iteration#011 COND#=+1.323307482483E+002, |dp|=+2.292179246183E-015
Iteration#012 COND#=+1.323307482483E+002, |dp|=+2.276281712951E-016
Iteration#013 COND#=+1.323307482483E+002, |dp|=+2.531400754737E-015
Iteration#014 COND#=+1.323307482483E+002, |dp|=+4.629134980199E-015
Iteration#015 COND#=+1.323307482483E+002, |dp|=+6.271020180030E-016
Iteration#016 COND#=+1.323307482483E+002, |dp|=+2.817118682949E-015
Iteration#017 COND#=+1.323307482483E+002, |dp|=+1.643911935350E-015
Iteration#018 COND#=+1.323307482483E+002, |dp|=+3.750478974854E-015
Iteration#019 COND#=+1.323307482483E+002, |dp|=+2.285941427087E-015
Iteration#020 COND#=+1.323307482483E+002, |dp|=+7.646224539136E-016
Iteration#021 COND#=+1.323307482483E+002, |dp|=+3.034966611429E-015
Iteration#022 COND#=+1.323307482483E+002, |dp|=+3.487456324109E-015
Iteration#023 COND#=+1.323307482483E+002, |dp|=+1.124162142583E-015
Iteration#024 COND#=+1.323307482483E+002, |dp|=+2.348696309578E-015
Iteration#025 COND#=+1.323307482483E+002, |dp|=+2.164764316289E-015
IPF Least Squares Filter Completed with Error |dp1| + |dp2| = +2.1647643162885121E-015
-----
```

Total Execution Time: 21 seconds

4 COMMENTS

Since this Course run only had a single science centroid, it should be used for sanity checking purposes, and to make first rough corrections to the focal plane quaternions.

1. Only two Brown angles (no Twist) were estimated associated with the frame table quaternion.
2. Overall the data set ran well and the filter converged properly. No modifications were required to the centroid CA file. The attitude AAfile also looked very clean with tracker and gyro working to spec.
3. The run was done in IPF Lite mode 2 (i.e., star tracker based attitude), for robustness and since high accuracy was not needed.
4. There were limitations in the experiment design due to only having a single science centroid and with a positive scan mirror angle. No centroids were available at the center or negative scan mirror positions to help sanity check polarities. This forced us to rely heavily on the polarities and plate/mirror scale parameters reported to us by MIPS team in calculating the alignment Brown angles.
5. Because only one science centroid was available, the final frame alignment error is no better than the science centroiding errors of 10" (in W) and 17" (in V), as reported in the CA file.
6. This run was made using BodyFrames_SPC_08a which was a special frame table incorporating the 40 star Stage 2 PAC filter run results.
7. There appears to be a slight discrepancy in the definition of all the Inferred frames in the provided FFfile and the current frame table BodyFrame_SPC_08a.xls (equivalent to BodyFrame_FTU_08a.xls). The Inferred frames in the FFfile are defined directly underneath each other in a straight vertical line, while their BodyFrame values are oriented at a slight angle.

We recommend updating frames 121, 113, 114, 116, 117, 122, 123, 125, 126 with the new quaternions listed in the IF file IF002121.dat. We realize these recommendations are large, being on the order of 1.5 arcminutes. However, our confidence in this change is on the order of at least 25 arcseconds.

The only caveat we have to this conclusion is if there was a gross error in the reported centroid, or geometry indicated in CA002121.m and/or CS002121.m files provided to the IPF filter. **Because of the size of the corrections, we strongly encourage the MIPS science team to review the integrity of the CA and CS files provided to us, before accepting our above conclusions.**

IPF TEAM CONTACT INFORMATION

IPF Team email	ipf@sirtfweb.jpl.nasa.gov	
David S. Bayard	X4-8208	David.S.Bayard@jpl.nasa.gov (TEAM LEADER)
Dhemetrio Boussalis	X4-3977	boussali@grover.jpl.nasa.gov
Paul Brugarolas	X4-9243	Paul.Brugarolas@jpl.nasa.gov
Bryan H. Kang	X4-0541	Bryan.H.Kang@jpl.nasa.gov
Edward.C.Wong	X4-3053	Edward.C.Wong@jpl.nasa.gov (TASK MANAGER)

ACKNOWLEDGEMENTS

This work was performed at the Jet Propulsion Laboratory, California Institute of Technology, under contract with the National Aeronautics and Space Administration.

References

- [1] D.S. Bayard, B.H. Kang, *SIRTF Instrument Pointing Frame Kalman Filter Algorithm*, JPL D-Document D-24809, September 30, 2003.
- [2] B.H. Kang, D.S. Bayard, *SIRTF Instrument Pointing Frame (IPF) Software Description Document and User's Guide*, JPL D-Document D-24808, September 30, 2003.
- [3] D.S. Bayard, B.H. Kang, *SIRTF Instrument Pointing Frame (IPF) Kalman Filter Unit Test Report*, JPL D-Document D-24810, September 30, 2003.
- [4] *Space Infrared Telescope Facility In-Orbit Checkout and Science Verification Mission Plan*, JPL D-Document D-22622, 674-FE-301 Version 1.4, February 8, 2002.
- [5] *Space Infrared Telescope Facility Observatory Description Document*, Lockheed Martin LMMS/P458569, 674-SEIT-300 Version 1.2, November 1, 2002.
- [6] *SIRTF Software Interface Specification for Science Centroid INPUT Files (CAFILER, CSFILE)*, JPL SOS-SIS-2002, November 18, 2002.
- [7] *SIRTF Software Interface Specification for Inferred Frames Offset INPUT Files (OFILE)*, JPL SOS-SIS-2003, November 18, 2002.
- [8] *SIRTF Software Interface Specification for PCRS Centroid INPUT Files (CBFILE)*, JPL SIS-FES-015, November 18, 2002.
- [9] *SIRTF Software Interface Specification for Attitude INPUT Files (AFILE, ASFILE)*, JPL SIS-FES-014, January 7, 2002.
- [10] *SIRTF Software Interface Specification for IPF Filter Output Files (IFFILE, LGFILE, TARFILE)*, JPL SOS-SIS-2005, November 18, 2002.
- [11] R.J. Brown, *Focal Surface to Object Space Field of View Conversion*. Systems Engineering Report SER No. S20447-OPT-051, Ball Aerospace & Technologies Corp., November 23, 1999.